LIMNOLOGY and OCEANOGRAPHY

ASLO

Limnol. Oceanogr. 66, 2021, 2563–2582

doi: 10.1002/lno.11773

Food web structure in relation to environmental drivers across a continental shelf ecosystem

Andrea Walters [1*] **Marianne Robert** [1] **Pierre Cresson** [2] **Hervé Le Bris** [3] **Dorothée Kopp** [1]

[1]IFREMER, Science and Halieutic Technology Research Unit, Lorient Cedex, France
[2]IFREMER, Channel and North Sea Fisheries Research Unit, Boulogne-sur-Mer, France
[3]ESE, Ecology and Ecosystem Health, Institut Agro, INRAE, Rennes, France

Abstract

Quantification of the physical and biological factors that influence the spatial structuring of food webs is central to inform effective resource management. We used baseline-corrected stable isotope ratios ($\delta^{13}C$ and $\delta^{15}N$) of 63 invertebrate and fish to investigate food web structure across a continental shelf gradient—the Celtic Sea Shelf in the Northeast Atlantic Ocean. Hierarchical clustering on $\delta^{13}C$ and $\delta^{15}N$ showed that the shelf food web is characterized by four trophic levels with trophic groups spread across pelagic and benthic trophic pathways. Four biomass-weighted isotopic diversity metrics provided indicators on the status of the system, showing a relatively complex food web with high trophic redundancy at intermediate trophic levels suggesting resilience to disturbances. Two sets of statistical models, at the community scale and for each trophic group, identified five distinct trophic assemblages associated with different chlorophyll *a* concentrations, water depth, and bottom temperature. A cold, vertically mixed-water assemblage over the outer shelf comprised the largest habitat and most diverse assemblage, highlighting the importance of cold productive conditions in the Celtic Sea. Trophic group model results were used to generate spatial area predictions to compare functioning of groups using isotopic overlap (similarity and nestedness) metrics. Isotopic niche area was larger (spanning two trophic levels) in shallow habitats, but not in habitats underlying high primary production or nutrient-rich water masses, suggesting stronger benthic-pelagic trophic coupling in inner shelf habitats. Results suggest that depth and intensity of pelagic production are major drivers of trophic structure and functioning of Celtic Sea communities.

Food web structure (i.e., the networks of trophic interactions that occur among species within ecosystems) is a fundamental feature of marine ecosystems as it affects energy transfer across trophic levels and biogeochemical cycles within and across ecosystems (Eddy et al. 2020). Understanding how marine food webs are structured along environmental gradients is essential to predict the response of ecosystems to the effects of global change, including anthropogenic pressures such as fishing on biodiversity. In addition, understanding the drivers of food web structure has been a key question in marine sciences: addressing the relationship between the intensity of primary production, usually inferred by the measurement of chlorophyll *a* concentration, and the production of biomass at high trophic levels is of prime importance, as mid- and high trophic level species largely enter global fisheries (Petrik et al. 2019). Biological transfer of carbon and other nutrients between the sea surface and deep waters may notably blur the link between pelagic primary production and benthic secondary production (Cresson et al. 2020; van Denderen et al. 2018), through the alteration of organic matter fluxes and organization of trophic niches among co-occurring species (Hayden et al. 2019). Human-induced anthropogenic impacts, such as fishing on benthic environments, can therefore have direct effects on demersal and pelagic systems and coupling strength between these systems (Agnetta et al. 2019).

Ecosystem models are an important tool to understand the effects of climate change and other anthropogenic activities across all trophic levels. However, they require reliable data inputs on food web linkages and overall food web structure (Seibold et al. 2018). Nitrogen ($\delta^{15}N$) and carbon ($\delta^{13}C$) stable isotope ratios are now recognized as efficient tracers of trophic fluxes in marine systems. The increase in $\delta^{15}N$ at each trophic level allows the use of this isotope ratio as a proxy of a consumers' trophic level. In contrast, $\delta^{13}C$ only slightly increases along the food web, and is thus commonly used to trace the origin of the production supporting the food web. For example, in marine systems globally, benthic food webs, whether

*Correspondence: arwalters38@gmail.com

Additional Supporting Information may be found in the online version of this article.

relying on macro- or microphytobenthic primary production, or on detrital matter, exhibit higher $\delta^{13}C$ values than pelagic ones based on the direct integration of phytoplanktonic production (Day et al. 2019; Hayden et al. 2019; Cresson et al. 2020). Combining both $\delta^{15}N$ and $\delta^{13}C$ has proven useful for illuminating the ecological structure and the organization of food webs within complex systems (Layman et al. 2012; Trueman et al. 2014; Giraldo et al. 2017). However, as the isotopic ratio of a consumer depends on the isotopic ratio of the production at the base of its food web, a consumer's ratio cannot be interpreted without knowledge about the trophic baseline. Addressing accurately the most reliable baseline value, whether with empirical measurements or statistical inferences (Jennings and Warr 2003; Jennings and van der Molen 2015) is one of the most important caveats in isotopic ecology, notably when investigating trophic patterns over large geographical scales. In addition, stable isotope derived metrics (i.e., Isotopic Functional Indices) have been recently demonstrated to be able to capture the trophic diversity and functioning of ecological systems. Under the premise that isotopic niche (the space occupied by organisms in a $\delta^{13}C$–$\delta^{15}N$ space) is a proxy of the trophic niche (e.g., Newsome et al. 2007), and including species biomass as a proxy of their importance (Cucherousset and Villéger 2015), indices can efficiently capture the trophic functioning of the system, notably by providing indicators of trophic redundancy or patchiness (Rigolet et al. 2015).

The Celtic Sea Shelf located in the Northeast Atlantic Ocean supports some of the largest and most important demersal and pelagic trawl fisheries in the region (Mateo et al. 2017; Moore et al. 2019). The shelf has undergone recent declines in the abundance of the large cold-water species (Atlantic cod *Gadus morhua*) in the area and an increase of small, noncommercial pelagic species (such as the boarfish *Capros aper*) has been documented in the area and elsewhere in the Northeast Atlantic (Pinnegar et al. 2002; Blanchard and Vandermeirsch 2005; McLean et al. 2019). To date, research into the Celtic Sea food web has predominantly focused on the trophic ecology of the fish community—demersal, benthic, and pelagic assemblages important in terms of biomass and fisheries in the Celtic Sea (Martinez et al. 2013) on the upper continental slope (Kopp et al. 2018), and along the shelf-wide gradient (Pinnegar et al. 2003; Rault et al. 2017; Day et al. 2019). However, there is little information on the overall structure of the food web in relation to the biophysical environment, which is central to understand the ecological consequences of changes in biophysical structuring of the system.

Within this context, the main objective of this study was to examine the physical and biological factors that influence the spatial structuring of the food web. Consistent with previous results obtained in neighboring or remote marine environments, we expected that depth and intensity of pelagic production would be major drivers of trophic structure and functioning of the Celtic Sea communities. For that purpose, we identified relationships between $\delta^{13}C$ and $\delta^{15}N$ baseline values and the environment to produce reliable estimates of trophic baseline and associated uncertainty to support robust comparisons of consumer trophic ecology across the shelf. Invertebrates (benthic macrofauna, zooplankton, and cephalopods) and fishes spanning a large trophic range from sites sampled across the spatial domain of the Celtic Sea were then used to assess spatial trends in $\delta^{13}C$ and $\delta^{15}N$ of organisms at higher trophic levels within the food web. The specific aims were to: (i) Characterize the food web structure at the scale of the whole sampling area (hereafter referred to as community scale) using a combination of hierarchical cluster analysis and four biomass-weighted isotopic diversity metrics (isotopic divergence, dispersion, evenness, and uniqueness; Cucherousset and Villéger 2015), (ii) identify biological and physical variables driving the trophic groups and the wider trophic network structure using two sets of statistical models, one set at the community scale and the other for each trophic group, to highlight the spatial structure of the food web, and (iii) compare functioning of trophic groups based on spatial areas identified using isotopic overlap (similarity and nestedness) metrics to identify underlying species assembly processes at different spatial scales.

Materials and Methods

Data collection

Sample collection

Samples were obtained during the EValuation Halieutique Ouest de l'Europe (EVHOE) surveys in November 2014, 2015, and 2016 (Duhamel et al. 2014; Leaute et al. 2015, 2016) as part of the International Bottom Trawl Surveys in the Celtic Sea (ICES 2015). A total of 975 samples of large epifaunal invertebrates (bivalve mollusks and decapod crustaceans), zooplankton (copepods), fish and cephalopod species corresponding to 63 species were collected and analyzed from water depths 57–306 m. Sample size varied between taxa (from 5 to 52), with an average of 15 individuals sampled per species (Table 1). Invertebrates and fish species were obtained by deploying a Grande Ouverture Verticale (GOV) demersal trawl with a cod-end of 20 mm stretched mesh, towed for 30 min at a speed of approximately 3.5 knots by R/V "Thalassa." As bottom trawls mostly target fish and cephalopods, the number of benthic invertebrates caught was small relative to total biomass of this fraction in the environment. Such observations are nonetheless particularly relevant as they represent the epi-benthic macrofauna—an important component at the base of the food web (Vaz et al. 2019). Copepods were sampled (November 2014) using a WP2 zooplankton net (Spartel, UK) with a 200 μm mesh size, towed (diagonally) at a speed of 0.75 m s^{-1} from the surface to 3 m above the seabed. Additional samples of the bivalve mollusk, the great scallop (*Pecten maximus*) were collected during professional fishing

Table 1. Names of all the studied Celtic Sea Shelf invertebrate and fish species, species codes and trophic groups used in next figures. The number of samples (*N*), mean $\delta^{13}C$ and $\delta^{15}N$ values (± SD) and estimated trophic level (TL ± SD) are listed for each species. Size of specimens is also given where available (carapace length for crustaceans, mantle length for cephalopods, and total length for fishes).

Trophic group	Code	Taxonomic class	Main position	*N*	$\delta^{13}C$ (‰) ± SD	$\delta^{15}N$ (‰) ± SD	TL ± SD	Size (cm) ± SD
Group 1. Pelagic primary consumers								
Copepods	CO	Hexanauplia	Pelagic	6	−21.06 ± 0.79	7.14 ± 0.88	2.08 ± 0.26	—
Sepia orbignyana	SO	Cephalopoda	Benthic	10	−19.85 ± 0.30	7.65 ± 1.00	2.23 ± 0.29	6.88 ± 1.04
Group 2. Benthic primary consumers								
Pecten maximus	PE	Bivalvia	Benthic	52	−17.47 ± 1.21	6.84 ± 1.76	2.00 ± 0.52	—
Group 3. Demersal/benthic fish & benthic cephalopods								
Sepia elegans	SE	Cephalopoda	Benthic	10	−19.53 ± 0.40	9.43 ± 1.01	2.76 ± 0.30	5.60 ± 2.37
Arnoglossus imperialis	AR	Actinopterygii	Benthic	10	−19.56 ± 0.75	8.83 ± 1.42	2.58 ± 0.42	13.80 ± 2.05
Callionymus maculatus	CM	Actinopterygii	Demersal	7	−20.24 ± 0.39	9.38 ± 1.75	2.74 ± 0.51	—
Capros aper	CA	Actinopterygii	Demersal	23	−19.53 ± 0.62	9.34 ± 1.74	2.73 ± 0.51	14.47 ± 1.28
Gadiculus argenteus argenteus	GA	Actinopterygii	Demersal	7	−19.64 ± 0.21	9.75 ± 0.29	2.85 ± 0.09	6.71 ± 0.76
Group 4. Pelagic/demersal/benthic fish, demersal cephalopods, & macrobenthos carnivores								
Munida intermedia	MU	Malacostraca	Benthic	6	−18.41 ± 0.84	9.15 ± 0.75	2.67 ± 0.22	1.40 ± 0.14
Sepiola sp.	SS	Cephalopoda	Demersal	16	−19.00 ± 0.48	11.49 ± 1.02	3.36 ± 0.30	—
Todaropsis eblanae	TO	Cephalopoda	Demersal	17	−19.14 ± 0.48	11.40 ± 1.52	3.33 ± 0.45	—
Clupea harengus	CL	Elasmobranchii	Demersal	10	−18.80 ± 1.52	11.23 ± 1.82	3.29 ± 0.54	22.90 ± 4.62
Eutrigla gurnardus	EU	Actinopterygii	Pelagic	10	−18.74 ± 0.91	10.81 ± 0.63	3.16 ± 0.18	21.15 ± 4.40
Helicolenus dactylopterus	HE	Actinopterygii	Demersal	7	−18.63 ± 0.15	10.49 ± 0.19	3.07 ± 0.06	14.00 ± 0.58
Lepidorhombus boscii	LE	Actinopterygii	Demersal	6	−19.11 ± 0.44	10.60 ± 0.47	3.10 ± 0.14	24.00 ± 2.65
Merluccius merluccius	ME	Actinopterygii	Benthic	39	−18.93 ± 0.68	12.22 ± 1.17	3.58 ± 0.34	26.85 ± 19.46
Micromesistius poutassou	MI	Actinopterygii	Demersal	26	−19.16 ± 0.44	11.19 ± 1.14	3.27 ± 0.34	27.42 ± 5.04
Phycis blennoides	PH	Actinopterygii	Pelagic	13	−19.02 ± 0.50	12.59 ± 0.76	3.68 ± 0.22	29.25 ± 8.78
Sardina pilchardus	SA	Actinopterygii	Demersal	12	−18.68 ± 0.78	10.20 ± 1.41	2.98 ± 0.41	17.00 ± 3.71
Scomber scombrus	SC	Actinopterygii	Pelagic	22	−19.02 ± 0.49	10.89 ± 1.19	3.18 ± 0.35	22.25 ± 4.80
Sprattus sprattus	SP	Actinopterygii	Pelagic	18	−18.31 ± 0.43	11.56 ± 0.64	3.38 ± 0.19	14.00 ± 2.89
Squalus acanthias	SQ	Actinopterygii	Pelagic	12	−19.47 ± 0.81	11.55 ± 1.51	3.38 ± 0.44	74.75 ± 16.39
Trisopterus esmarkii	TR	Actinopterygii	Demersal	14	−19.18 ± 0.47	12.07 ± 1.14	3.53 ± 0.34	19.88 ± 2.30
Group 5. Demersal/benthic fish, demersal cephalopods, & macrobenthos carnivores								
Macropipus tuberculatus	MC	Malacostraca	Benthic	12	−18.52 ± 1.12	10.82 ± 2.02	3.16 ± 0.59	—
Nephrops norvegicus	NE	Malacostraca	Benthic	18	−17.71 ± 0.90	10.59 ± 1.15	3.10 ± 0.34	7.50 ± 1.41
Illex coindetii	IL	Cephalopoda	Demersal	19	−18.72 ± 0.93	11.42 ± 1.49	3.34 ± 0.44	—
Rossia macrosoma	RO	Cephalopoda	Demersal	12	−18.32 ± 0.47	10.96 ± 1.81	3.21 ± 0.53	—
Callionymus lyra	CR	Elasmobranchii	Benthic	14	−17.85 ± 0.91	11.33 ± 1.13	3.31 ± 0.33	22.71 ± 2.58
Glyptocephalus cynoglossus	GL	Actinopterygii	Demersal	10	−17.97 ± 0.78	11.74 ± 1.18	3.43 ± 0.35	36.00 ± 5.83
Hippoglossoides platessoides	HI	Actinopterygii	Benthic	7	−18.30 ± 1.81	11.69 ± 0.34	3.42 ± 0.10	22.71 ± 1.50
Lepidorhombus whiffiagonis	LW	Actinopterygii	Benthic	27	−18.51 ± 0.93	10.52 ± 1.49	3.08 ± 0.44	23.81 ± 11.72
Leucoraja naevus	LN	Actinopterygii	Benthic	10	−17.74 ± 0.89	11.52 ± 1.53	3.37 ± 0.45	56.50 ± 9.70
Lophius piscatorius	LO	Actinopterygii	Demersal	29	−18.21 ± 0.66	11.76 ± 1.76	3.44 ± 0.52	35.24 ± 21.56
Microstomus kitt	MK	Actinopterygii	Benthic	12	−17.61 ± 1.45	10.39 ± 1.89	3.04 ± 0.56	27.42 ± 5.04
Group 6. Pelagic/demersal fish & demersal cephalopods								
Alloteuthis sp.	AL	Cephalopoda	Demersal	13	−18.46 ± 0.94	12.90 ± 1.51	3.78 ± 0.44	—
Loligo forbesii	LF	Cephalopoda	Demersal	19	−18.21 ± 0.69	12.88 ± 1.07	3.77 ± 0.31	15.53 ± 10.98

(Continues)

Table 1. Continued

Trophic group	Code	Taxonomic class	Main position	*N*	$\delta^{13}C$ (‰) ± SD	$\delta^{15}N$ (‰) ± SD	TL ± SD	Size (cm) ± SD
Argentina sphyraena	AS	Actinopterygii	Demersal	17	−18.66 ± 0.93	11.88 ± 2.31	3.48 ± 0.68	17.47 ± 3.06
Chelidonichthys cuculus	CH	Actinopterygii	Demersal	19	−17.82 ± 1.17	13.02 ± 1.81	3.81 ± 0.53	24.05 ± 2.44
Conger conger	CC	Actinopterygii	Demersal	6	−18.30 ± 1.04	13.55 ± 1.26	3.97 ± 0.37	106.83 ± 26.48
Engraulis encrasicolus	EN	Actinopterygii	Pelagic	8	−17.86 ± 0.66	12.24 ± 1.18	3.58 ± 0.35	12.13 ± 3.52
Lophius budegassa	LB	Actinopterygii	Demersal	27	−18.45 ± 0.75	12.66 ± 1.43	3.71 ± 0.42	18.96 ± 8.52
Melanogrammus aeglefinus	MA	Actinopterygii	Demersal	39	−18.05 ± 1.18	12.82 ± 1.26	3.75 ± 0.37	24.95 ± 7.24
Mullus surmuletus	MS	Actinopterygii	Demersal	11	−17.72 ± 0.70	13.24 ± 0.93	3.88 ± 0.27	17.07 ± 5.15
Trachurus trachurus	TT	Actinopterygii	Pelagic	27	−18.54 ± 0.79	12.44 ± 1.73	3.64 ± 0.51	20.95 ± 10.63
Trisopterus minutus	TM	Actinopterygii	Demersal	20	−18.45 ± 1.35	12.26 ± 2.35	3.59 ± 0.69	16.89 ± 3.35
Group 7. Demersal predatory fish								
Gadus morhua	GM	Actinopterygii	Demersal	36	−17.14 ± 0.63	14.95 ± 0.67	4.38 ± 0.20	58.25 ± 23.72
Merlangius merlangus	MM	Actinopterygii	Demersal	34	−18.02 ± 0.64	13.71 ± 0.71	4.02 ± 0.21	25.06 ± 7.22
Molva molva	MO	Actinopterygii	Demersal	8	−17.78 ± 0.53	14.19 ± 1.27	4.16 ± 0.37	61.00 ± 6.78
Zeus faber	ZE	Actinopterygii	Demersal	14	−17.41 ± 0.18	14.02 ± 1.02	4.11 ± 0.30	36.07 ± 10.09
Group 8. Demersal/benthic fish & macrobenthos carnivores								
Cancer pagurus	CP	Malacostraca	Benthic	8	−16.48 ± 0.72	11.30 ± 1.32	3.30 ± 0.39	18.10 ± 0.85
Maja brachydactyla	MB	Malacostraca	Benthic	6	−15.63 ± 0.45	10.85 ± 1.21	3.17 ± 0.36	14.00 ± 0.00
Chelidonichthys lucerna	CS	Elasmobranchii	Demersal	5	−16.01 ± 0.45	13.05 ± 1.26	3.82 ± 0.37	-
Dicentrarchus labrax	DI	Elasmobranchii	Benthic	8	−16.67 ± 0.51	13.99 ± 1.26	4.10 ± 0.37	52.00 ± 5.57
Limanda limanda	LI	Elasmobranchii	Benthic	8	−16.74 ± 0.66	12.22 ± 1.45	3.58 ± 0.43	23.33 ± 2.08
Microchirus variegatus	MV	Elasmobranchii	Benthic	16	−17.27 ± 0.87	12.41 ± 1.89	3.63 ± 0.56	15.44 ± 1.63
Mustelus asterias	MT	Elasmobranchii	Demersal	14	−16.23 ± 0.76	12.86 ± 1.28	3.76 ± 0.38	88.22 ± 13.95
Pleuronectes platessa	PL	Actinopterygii	Demersal	26	−16.51 ± 0.60	13.15 ± 1.34	3.85 ± 0.39	31.15 ± 5.84
Scophthalmus maximus	SM	Actinopterygii	Demersal	7	−17.01 ± 0.38	13.25 ± 0.97	3.88 ± 0.29	56.67 ± 5.69
Raja clavata	RC	Actinopterygii	Benthic	7	−16.68 ± 1.09	11.74 ± 0.89	3.44 ± 0.26	56.00 ± 7.07
Raja microocellata	RA	Actinopterygii	Benthic	6	−16.07 ± 0.50	12.14 ± 0.43	3.55 ± 0.13	69.80 ± 12.17
Raja montagui	RM	Actinopterygii	Benthic	10	−15.94 ± 0.40	12.89 ± 0.55	3.77 ± 0.16	54.20 ± 5.50
Scyliorhinus canicula	SN	Actinopterygii	Benthic	14	−16.96 ± 0.78	12.80 ± 1.40	3.75 ± 0.41	63.36 ± 5.61
Solea solea	SL	Actinopterygii	Benthic	19	−17.20 ± 0.74	12.54 ± 1.10	3.67 ± 0.32	30.74 ± 7.73

operations (November 2015). All samples were kept frozen at −20°C until processing in the laboratory.

Stable isotope analysis

Fish were measured for total length (cm) and a sample of white dorsal muscle tissue was dissected. For invertebrates, sample processing varied according to taxon. A tissue sample was taken from the muscle of crustaceans, from the abductor muscle of bivalve mollusks, and from the mantle of cephalopods. Copepods were prepared whole. After dissection, all samples were washed in distilled water to prevent contamination by sediment carbonates, dried for 48 h at 60°C and homogenized into a powder using a mixer mill (Model MM400, Retsch, Germany). Carbon ($^{13}C/^{12}C$, $\delta^{13}C$) and nitrogen ($^{15}N/^{14}N$, $\delta^{15}N$) stable isotope composition, and % content of C and N of the powdered samples was determined using a Carlo Erba NC2500 Elemental Analyzer by the Stable Isotopes in Nature Laboratory (SINLAB, University of New Brunswick, Canada). Data were corrected using three reference samples of SINLAB standards (bass muscle, bovine liver and nicotinamide; SD < 0.2‰ for $\delta^{13}C$ and < 0.1‰ for $\delta^{15}N$). Reference materials were previously calibrated against interlaboratory comparison standards distributed by the International Atomic Energy Agency (IAEA). The ^{13}C composition of the tissue samples was expressed in conventional delta notation ($\delta^{13}C$), relative to the abundance of ^{13}C in Pee Dee Belemnite and the ^{15}N composition ($\delta^{15}N$) relative to the abundance of ^{15}N in atmospheric N_2. For most taxa, the mean observed C:N ratio was lower than 3.5 (the value above which lipid normalization is recommended; Post et al. 2007), except for copepods, the cephalopod *Sepiola* sp., European common squid *Alloteuthis* sp., European sprat *Sprattus sprattus* and the striped red mullet *Mullus surmuletus*. Normalization of $\delta^{13}C$

data of these invertebrate and fish taxa was performed using the mass balance equations in Smyntek et al. (2007) and Barnes et al. (2009), respectively.

Trophic baseline and trophic levels of taxa

Sedentary filter-feeding consumers integrate local temporal variation in $\delta^{13}C$ and $\delta^{15}N$ providing a time-averaged isotopic signal that is more stable than that of primary producers (Post 2002). Filter-feeders are thus often used as tracers of stable isotope baseline variations (Lorrain et al. 2002; Jennings and Warr 2003). We used the widely distributed great scallop (*P. maximus*; Supporting Information Fig. S1) to provide a realistic trophic baseline estimate for the majority of taxa in this study, which we expect to rely upon a mixture of both benthic and pelagic food sources (Rault et al. 2017; Kopp et al. 2018; Day et al. 2019). Following the studies of Barnes et al. (2009) and Jennings and van der Molen (2015) conducted in the same ecosystem, invertebrate and fish $\delta^{13}C$ and $\delta^{15}N$ were corrected for spatial variation in the isotopic baseline based on environmental data as follows:

$$\delta^{13}C_{base,i} = 0.322T_i - 20.347$$

$$\delta^{15}N_{base,i} = b_0 + b_1 T_i + b_2 S_i + b_3 S_{\min,i} + b_4 T_i S_i + \epsilon_i$$

where $\delta^{13}C_{base,i}$ and $\delta^{15}N_{base,i}$ are the corrected baseline $\delta^{13}C$ and $\delta^{15}N$ values, respectively, for the individual i, T, and S are annual mean bottom temperature and salinity, respectively, $S_{\min}$ is minimum monthly salinity, and b_0, b_1, b_2, b_3, b_4 are the fit statistics used to simulate uncertainty in $\delta^{15}N_{base}$ (Jennings and van der Molen 2015). Errors were assumed to have a constant variance. Annual mean bottom temperature was obtained from the Iberian Biscay Irish, IBM, Ocean Reanalysis system, and annual mean bottom salinity and minimum monthly salinity was provided by the Copernicus Marine environment monitoring service, CMEMS, at http://marine.copernicus.eu). All stable isotope data used in further analyses are baseline-corrected stable isotope data.

Having corrected for spatial variation in $\delta^{13}C_{base}$ and $\delta^{15}N_{base}$, we used the method established by Post (2002) to estimate trophic levels for taxa:

$$TL_i = \lambda_{base} + \left[\left(\delta^{15}N_i - \delta^{15}N_{base}\right)/\Delta^{15}N\right]$$

where λ_{base} is the corresponding base trophic level (TL), assumed here to be 2, $\delta^{15}N_i$ is the corrected $\delta^{15}N$ value for the individual i, and $\delta^{15}N_{base}$ is the mean of all *P. maximus* corrected $\delta^{15}N$ values. We used a fractionation factor ($\Delta^{15}N$) of 3.4 (Post 2002) as the average ^{15}N enrichment between the muscle tissue of fishes and invertebrates, and *P. maximus* as the base trophic level. The trophic level for a species was then calculated by averaging the individual trophic levels.

Biological and physical predictors

Four variables were analyzed as possible explanatory variables of trophic variability across the Celtic Sea: chlorophyll *a* concentration, bottom temperature, water depth and seabed substrate (Fig. 1). Seabed substrate data were obtained from the European Marine Observation and Data network (EMODnet) Seabed Habitats platform at http://www.emodnet.eu/seabed-habitats (Populus et al. 2017). Mean annual chlorophyll *a* concentration derived from ESA Ocean Color CCI Remote Sensing Reflectance data were provided by CMEMS (Gohin et al. 2008; Hu et al. 2012). Bathymetry data in Fig. 1a were obtained from the ETOPO2 dataset (National Geophysical Data Center 2006), implemented in R 4.0.2 (R Core Team 2020) with the package *raadtools* version 0.5.2.9003 (Sumner 2019). Annual mean bottom temperature and chlorophyll *a* data was selected to reflect the relatively long turnover time (several months or more) of $\delta^{15}N$ and $\delta^{15}N$ in the tissues of bivalve mollusks (Lorrain et al. 2002; Jennings and Warr 2003). Environmental predictor variables were extracted for each pixel of the spatial domain and averaged across the temporal range of sampled location data (2014–2016). The locations of satellite and remote sensing data were then matched with stable isotope data to the nearest tenth of a decimal degree using latitude and longitude of each sampled site.

Data analysis

Characterization of food web and trophic groups of species

In order to characterize the food web structure, hierarchical clustering (via Euclidean distances and the Ward method) was used to distinguish clusters of species according to their $\delta^{13}C$ and $\delta^{15}N$ values, which is a commonly used approach for this type of data (e.g., Kopp et al. 2015). To account for within-sample variation in isotopic values, hierarchical clustering was performed on a bootstrapped matrix of distances between species, implemented via the R package *vegan* version 2.5–6 (Oksanen et al. 2019). Since the minimum sample size was 5, five individuals per species were randomly sampled via the Simple Random Sampling With Replacement method. The isotopic data of these samples were then used to generate Euclidean distance matrices between species using 500 iterations. The resulting distance matrices were averaged to obtain the bootstrapped distance on which clustering was performed. The optimal number of clusters was assessed by visual inspection of the resulting dendrogram (*see* Supporting Information Fig. S2) and confirmed using graphs of fusion level (Borcard et al. 2018). Analysis of Similarities (ANOSIM) was used to determine whether clusters were significantly different. Trophic increases of +1‰ in $\delta^{13}C$ and +4.5‰ in $\delta^{15}N$ and of +2‰ in $\delta^{13}C$ and +2.5‰ in $\delta^{15}N$ were used to show the ranges of isotopic ratios expected for trophic transfer of pelagic and benthic organic matter, respectively (Darnaude et al. 2004). The isotopic ratios of a pelagic primary consumer (copepods) and of a benthic primary consumer (*P. maximus*) were used as a starting point of the range for the pelagic and benthic trophic pathway, respectively. All mean values are presented with standard deviation unless stated otherwise. The characterization of taxa (benthic, demersal, or pelagic) and the naming of resulting trophic groups were made based on scientific literature analysis of their feeding habits (preference for northern Europe studies), site (coastal zones not including estuaries), substrate (soft bottom),

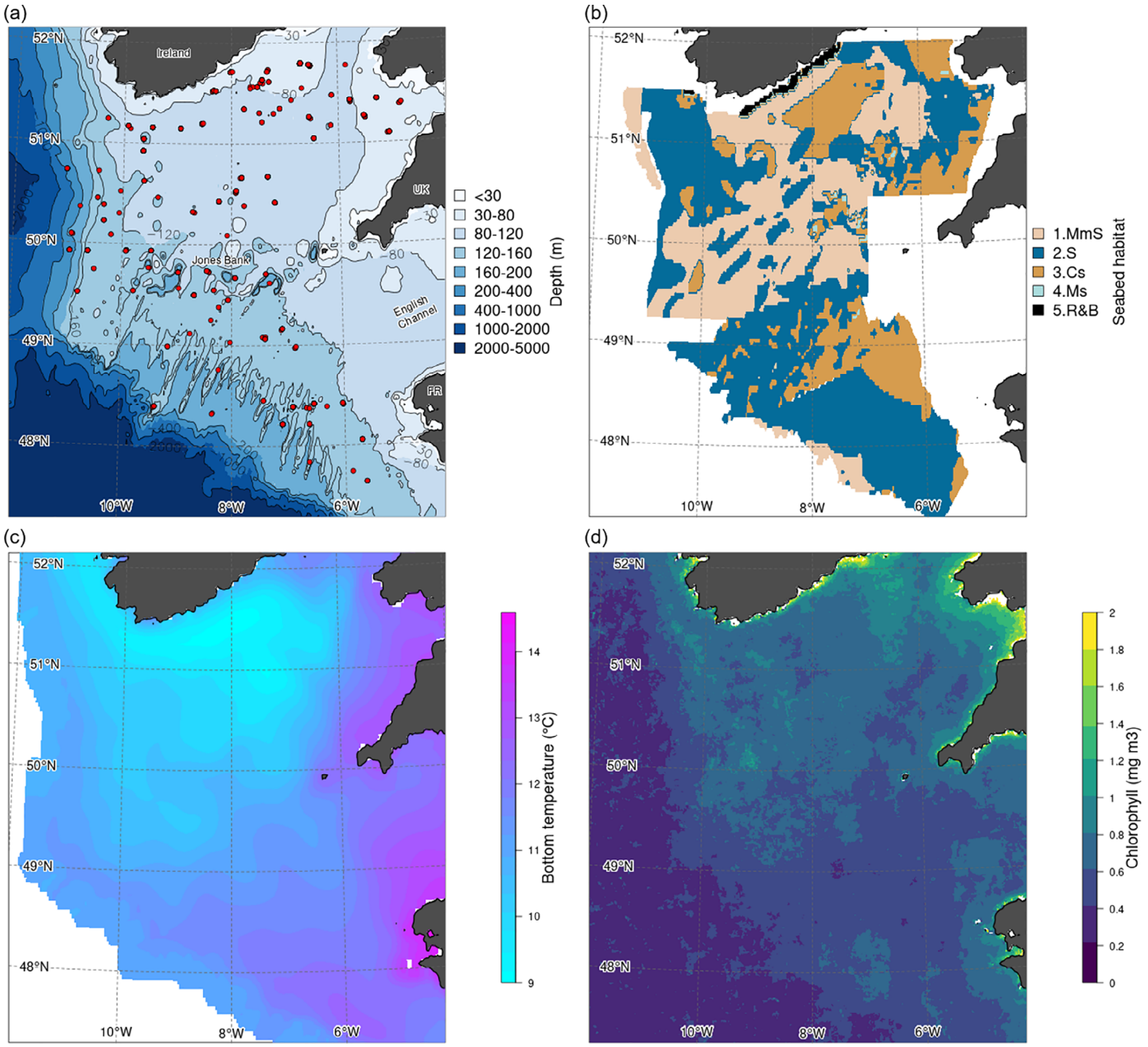

Fig 1. (**a**) Spatial extent of sampling on the Celtic Sea Shelf. Isobaths (black lines) are shown at 30, 80, 120, 160, 200, 400, 1000, 2000, and 4000 m depth intervals. Red circles identify sampling locations. (**b**) Broad-scale seabed habitat classification as compiled by EMODnet. 1. MmS = mud to muddy sand, 2. S = sand, 3. Cs = coarse substrate, 4. Ms = mixed sediment, 5. R&B = rocky and boulders. (**c**) Mean annual bottom temperature, and (**d**) chlorophyll *a* concentration in surface waters averaged across the temporal range of sampled location data (2014–2016).

species size (considering ontogenetic shifts in diet), and season (autumn). Details of taxa and trophic group assignments are provided in the Supporting Information (Table S1).

Quantifying isotopic diversity metrics for the food web

Four isotopic diversity metrics (isotopic divergence, dispersion, evenness, and uniqueness) were used to examine trophic structure in the Celtic Sea (*see* Cucherousset and Villéger 2015 and references therein for specific details on these metrics including equations for calculations): (a) Isotopic divergence indicates the degree to which species distribution in the isotopic space maximizes the trophic divergence within the food web. Low isotopic divergence (i.e., tends to 0) indicates that relative biomasses are dominated by more generalist species

(i.e., species closer to the center of gravity of the convex hull). Conversely, high isotopic divergence (i.e., tends to 1) indicates that species with the highest biomass occupy the isotopic space more densely on the edges of the convex hull, revealing a trophic specialization and thus a high degree of niche differentiation in the food web. (b) Isotopic dispersion indicates the average trophic diversity in the food web. Isotopic dispersion equals 0 when all species have the same isotope values and increases to 1 when most of the points (or their weight) are far from the center of gravity of the group of points. (c) Isotopic evenness indicates the regularity in species distribution and the density in species packing in the occupied isotopic space. Low isotopic evenness index (i.e., tends to 0) indicates that the food web is composed of clusters of species and implies trophic redundancy and competition for food. In contrast, high isotopic evenness (i.e., tends to 1) indicates that species and relative biomasses are evenly distributed in the isotope space, resulting in higher functional regularity and allowing optimal resource use through niche partitioning (Rigolet et al. 2015). (d) Isotopic uniqueness is defined as the inverse of the average isotopic redundancy (i.e., the average closeness of species in the isotope space). Isotopic uniqueness equals 0 when each species has at least one species with the same position in the isotope space (i.e., clustering of species with similar diets) and tends to 1 when most species (or species with the highest biomass) are isolated in the isotope space.

Diversity metrics required the calculation of convex hull area fitted over species mean $\delta^{13}C$ and $\delta^{15}N$ values. It gives an indication of the extent of the isotopic niche space of the entire trophic network structure and provides information on how the isotopic functional space (i.e., total area of the convex hull) is filled by species (Cucherousset and Villéger 2015). Biomass indices are also required. They are based on species collected during the EVHOE surveys. Biomass indices for each species at each station were raised (based on a depth zonation stratification) to the spatial domain of the Celtic Sea. Copepod sampling was insufficient to produce reliable biomass estimates and were subsequently precluded from all further analyses. Metrics were implemented via the R packages *geometry* version 0.4.5 (Habel et al. 2019) and *ape* version 5.0 (Paradis and Schliep 2019).

Isotopic space in relation to the environment

As relationships with biological and physical variables were not expected to be linear, we used generalized additive models (GAMs), with a Gaussian distribution and identity link function, implemented via the R package *mgcv* version 1.8–31 (Wood 2017). To assess isotopic space in relation to the biophysical environment, we fitted community scale- and trophic group-specific GAMs separately on $\delta^{13}C$ and $\delta^{15}N$ data. Predictor variables were scaled and centered to account for the different scales of measurement, and all models included a spatial autocorrelation structure to account for the spatial dependence in the data. Model selection was determined by manually running different combinations of covariates in a stepwise process beginning with a model fitted for each of the covariates separately (in addition to the spatial auto-correlation term). The top model of this set of single term models was selected based on Akaike's Information Criterion (AICc) for small sample sizes (Burnham and Anderson 2002). A set of two-term models was then run, including this top model plus each of the remaining three variables. If the top two-term model resulted in improved performance in terms of AICc (ΔAICc) and percent deviance explained (Δ% dev), a set of three-term models was then run, and so on up to the four variables. As the sample size of trophic group 3 (demersal/benthic fish & benthic cephalopods) was smaller than the number of covariates preventing model convergence, comparison of isotopic trends and the environment could not be assessed for this group.

Overlap indices of trophic groups based on areas identified using GAMs

To better infer the spatial effect of environmental conditions on the functioning of trophic groups, two isotopic overlap metrics (isotopic similarity and isotopic nestedness; Cucherousset and Villéger 2015 and references therein) were used to compare the position and size of the isotopic niche among trophic groups associated with key predictor variables across the Celtic Sea. The degree of isotopic overlap was quantified based on spatial areas identified from trophic group models. For selected trophic groups, we first extracted the $\delta^{13}C$ and $\delta^{15}N$ data for each species at each station across the spatial areas identified to create trophic groups per spatial area. Biomass indices for each species at each station were raised to the spatial area surface (instead of the whole shelf domain) to create species biomass indices per spatial area. Isotopic overlap metrics were quantified using the total convex hull areas of two groups and the volume of isotopic space they shared (i.e., volume of their intersection). Isotopic similarity equals 0 when the two groups of organisms fill totally different parts of the stable isotope space and increases to 1 when they fill the same portion of the stable isotope space. Isotopic nestedness equals 0 when there is no isotopic overlap and increases to 1 when the group with the smallest convex hull fills a subset of the isotopic space filled by the group with the largest convex hull.

Results

Structure of the food web

Mean $\delta^{15}N$ values ranged from 6.84‰ to 14.95‰ with the bivalve mollusk, *P. maximus*, showing the lowest $\delta^{15}N$ values, and the large predatory fish, Atlantic cod *G. morhua*, the highest values (Table 1). Mean trophic level estimates spanned three trophic levels from *P. maximus* and copepods (trophic level 2) to demersal predatory fishes (trophic level 4.4, Table 1; Fig. 2). Mean $\delta^{13}C$ values ranged from −21.06‰ to

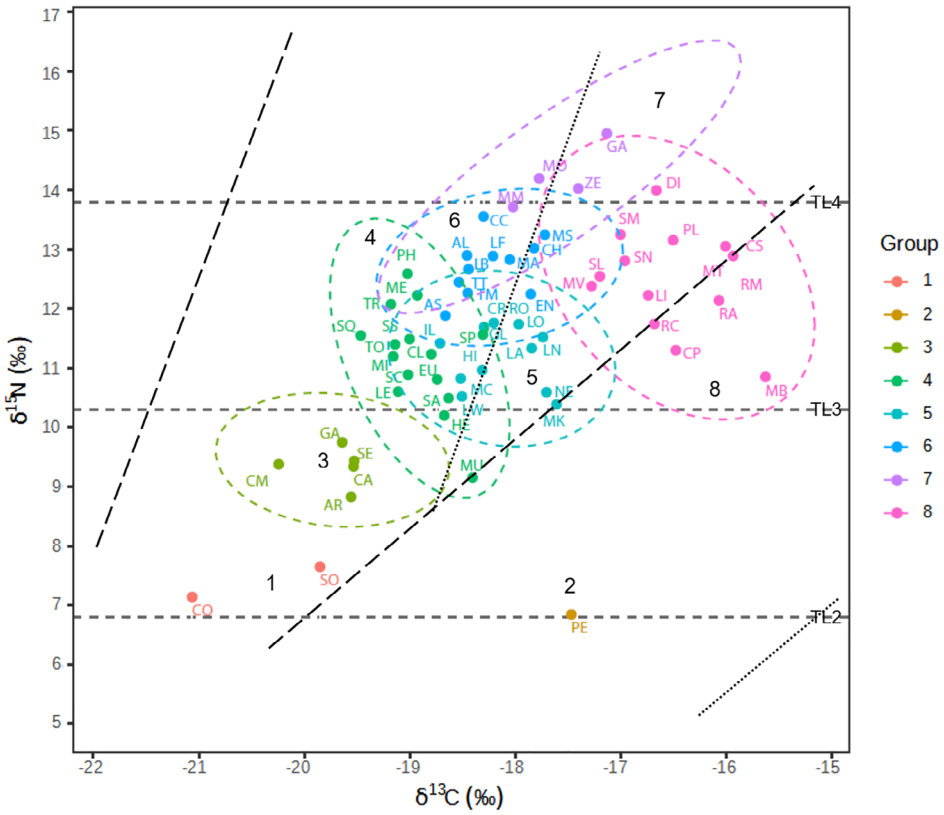

Fig 2. Mean $\delta^{13}C$ and $\delta^{15}N$ values for Celtic Sea Shelf invertebrates and fishes; color denotes trophic groups 1–8 resulting from the hierarchical clustering analyses, with ellipses showing 95% confidence interval values for each trophic group with sufficient data points. Scientific names corresponding to species codes are given in Table 1; gray dashed lines show median $\delta^{15}N$ values for each approximate trophic level (TL) 2–4 from low to high on the y-axis. Large black dashed and small black dotted lines show the limits of the ranges of isotopic ratios expected for trophic transfer of pelagic and benthic organic matter, respectively. Data from all years combined.

– 15.63‰. The $\delta^{13}C$ values varied greatly among primary consumers with *P. maximus* exhibiting relatively high values compared to copepods.

Hierarchical clustering analyses of $\delta^{13}C$ and $\delta^{15}N$ of species distinguished eight clusters (ANOSIM, $r = 0.40$, $p < 0.001$; Table 1; Fig. 2) corresponding to various trophic groups. Group 1, named "Pelagic primary consumers" is represented by copepods, and by the pink cuttlefish *Sepia orbignyana*. Group 2, "Benthic primary consumers" is only represented by the bivalve mollusk, *P. maximus*. Above these primary consumers, various groups follow one another to the top of the food web: group 3, "Demersal/benthic fish & benthic cephalopods" (one cephalopod and four fish), group 4,"Pelagic/demersal/benthic fish, demersal cephalopods & macrobenthos carnivores" (one crustacean decapod, two cephalopods and 12 fish), group 5, "Demersal/benthic fish, demersal cephalopods & macrobenthos carnivores" (two crustacean decapods, two cephalopods, and nine fish), is positioned at the same trophic level as group 4, but is less ^{13}C depleted, marking the benthic pathway (Fig. 2), whereas group 4 is positioned more on the pelagic pathway. Following at a higher trophic level is group 6, "Pelagic/demersal fish & demersal squid" (two cephalopods and nine fish). At the top of the food web, group 7, "Demersal predatory fish" (four fish) is composed of large fish species (Table 1). Finally, group 8, "Demersal/benthic fish & macrobenthos carnivores" (two crustacean decapods and 12 fish), is situated at the same trophic level as group 6, but is less ^{13}C depleted (Fig. 2). As seen between groups 4 and 5 at a lower trophic level, group 8 is positioned on the benthic pathway while group 6 is on the pelagic one.

Biomass-weighted values influenced the distribution of points within the convex hull (Fig. 3). Group 3 was characterized by a very high biomass of fish species, namely boarfish (*C. aper*). Above group 3 on the scaled $\delta^{15}N$ axis, group 4 was dominated by two pelagic fish: Atlantic herring (*Clupea harengus*) and mackerel (*Scomber scombrus*) as well as the demersal fish, the Norway pout (*Trisopterus esmarkii*). The biomass of group 5 was dominated by the neritic demersal cephalopod species southern shortfin squid (*Illex coindetii*), while the pelagic horse mackerel (*T. trachurus*) and the demersal poor cod (*Trisopterus minutus*) had the highest biomasses in group 6. Larger-bodied demersal fish, the whiting (*Merlangius*

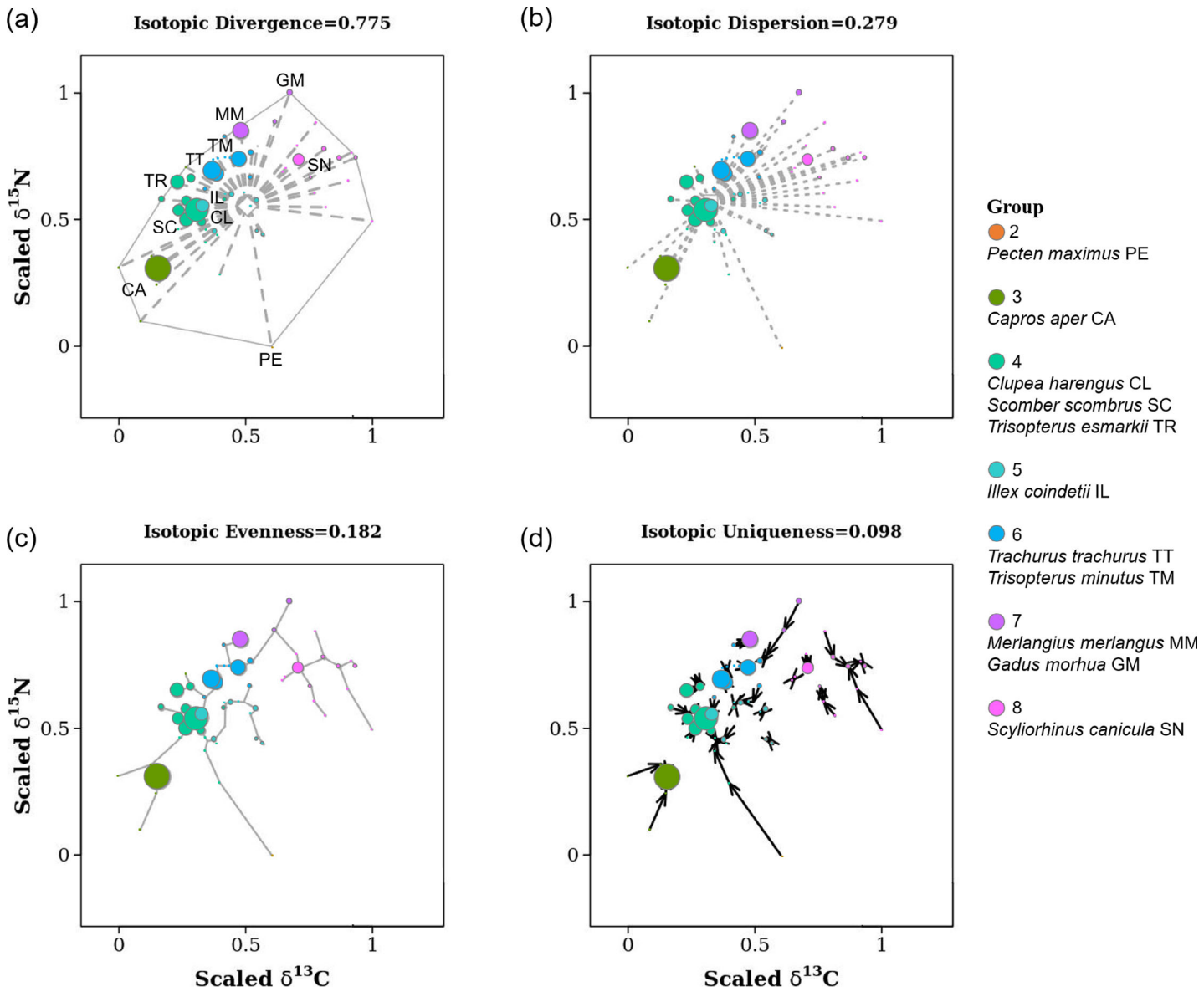

Fig 3. Stable isotope diversity metrics for the Celtic Sea Shelf trophic network. Points represent the isotopic position of each species (weighted by biomass) in a scaled (0–1) $\delta^{13}C$–$\delta^{15}N$ space. Color denotes trophic groups 2–8 resulting from the hierarchical clustering analyses. Species with the largest biomass in each trophic group are listed in the legend and displayed with species codes. (**a**) Isotopic divergence, distribution of species importance within the border of the convex hull (open polygon shape). (**b**) Isotopic dispersion, weighted-mean distance (dashed lines) to the Center of gravity of all points. (**c**) Isotopic evenness, regularity in the distribution of points along the shortest tree linking all the points (solid lines). (**d**) Isotopic uniqueness, weighted-mean of distances to nearest neighbor (black arrows).

merlangus) and lesser-spotted dogfish (*Scyliorhinus canicula*), had the highest biomasses in groups 7 and 8, respectively.

In the Celtic Sea Shelf ecosystem, species with the highest biomass occupied the isotopic space more densely on the edges of the convex hull (high Isotopic Divergence of 0.775, Fig. 3a), indicating a trophic specialization and thus a high degree of niche differentiation in the food web. Average trophic diversity in the food web was low (Isotopic Dispersion of 0.279, Fig. 3b), with most of the biomass centered on groups 4–6, which lay at the center of gravity of the group of points. This in turn highlights the low biomass of large top predatory fish (e.g., Atlantic cod *G. morhua*), which lay far from the center of points (Fig. 3b), and the increased biomass of smaller-bodied pelagic and demersal fish species feeding within trophic level 3 (Fig. 2). Low Isotopic Evenness of 0.182 (Fig. 3c) indicates that the food web is composed of clusters of species (i.e., packed species) and implies trophic redundancy and substantial competition for food, especially between bentho-

demersal fish, cephalopods, and macrobenthos (i.e., groups 4 and 5, respectively). Accordingly, distance between the species points (as indicated by the size of the arrows in Fig. 3d) was smaller among groups 4–8 compared to group 3, indicating that each species has at least one species with the same position in the isotope space (i.e., clustering of species with similar diets) and implies high trophic redundancy within trophic level 3 (low Isotopic Uniqueness of 0.098, Fig. 3d).

Isotope space in relation to the environment

At the community scale, the model including chlorophyll *a* and depth had the best predictive ability explaining 43.7% of the deviance in the $\delta^{13}C$ data (Table 2; Supporting Information Table S2). A positive association with higher $\delta^{13}C$ values was evident between a chlorophyll *a* of 0.6 and 0.8 mg m^{-3} and shallower bathymetry (< 80 m depth; Fig. 4a), which in this study corresponded well with colder bottom temperatures (< 11°C) on the outer shelf (i.e., the area extending north from the central part of the study area over the Jones Bank) and stations surveying the northeast inner shelf (Fig. 1a,c). For $\delta^{15}N$, the model including chlorophyll *a* and bottom temperature had the best predictive ability explaining 42.3% of the deviance in the data (Table 2; Supporting Information Table S1). The smoothed relationships indicated a higher probability of elevated $\delta^{15}N$ values in areas of moderate chlorophyll *a* (between 0.6 and 0.8 mg m^{-3}), indicating a similar spatial patterning for $\delta^{13}C$ and $\delta^{15}N$ values over the outer shelf (Figs. 4a, 5a). A positive association with higher $\delta^{15}N$ values was also evident in areas characterized by warmer bottom temperatures (> 11.5°C), which corresponded to sampling sites over the northeast inner shelf (< 80 m depth) and southern parts of the survey area (Fig. 1c,d).

We fitted trophic group-specific GAMs to $\delta^{13}C$ and $\delta^{15}N$ on six groups with enough data. Model predictive ability was good for groups 2, 5, 6, and 8 with percentage of deviance explained ranging from 58.0% to 88.0% (Table 2). Models for group 4 and 7 had poorer fits, explaining 37.1% and 35.0% of the deviance in the data, respectively. For each group, the best model fitted to $\delta^{13}C$ included one or two predictor variables (Table 2). The $\delta^{13}C$ values of group 2 were influenced by bottom temperature (Fig. 4b), with higher $\delta^{13}C$ values, on average, in areas with colder bottom temperatures (< 10.4°C),

Table 2. Summary of generalized additive models (GAMs) of the relationship between the most explanatory environmental variables and $\delta^{13}C$ and $\delta^{15}N$ for (**a**) community scale models and (**b**–**g**) trophic group models. BotTemp, bottom temperature; CHLa, chlorophyll *a* concentrations, DEPTH = water depth; seaHab, seabed habitat; (lon,lat) = spatial auto-correlation term. Trophic groups 2, 4–8 as in Table 1.

	Model formula	N. terms	N. obs	% dev	r^2
1. Carbon ($\delta^{13}C$)					
(a) Community scale	$\delta^{13}C$ ~ CHLa + DEPTH + (lon,lat)	2	114	43.7	0.425
(b) Benthic primary producers (group 2)	$\delta^{13}C$ ~ BotTemp + (lon,lat)	1	23	88.6	0.866
(c) Pelagic/demersal/benthic fish, demersal cephalopods & macrobenthos carnivores (group 4)	$\delta^{13}C$ ~ CHLa + (lon,lat)	1	48	37.1	0.336
(d) Demersal/benthic fish, demersal cephalopods & macrobenthos carnivores (group 5)	$\delta^{13}C$ ~ seaHab + (lon,lat)	1	50	58.3	0.563
(e) Pelagic/demersal fish & demersal cephalopods (group 6)	$\delta^{13}C$ ~ CHLa + DEPTH + (lon,lat)	2	33	68.6	0.667
(f) Demersal predatory fish (group 7)	$\delta^{13}C$ ~ CHLa + (lon,lat)	1	25	35.0	0.287
(g) Demersal/benthic fish & macrobenthos carnivores (group 8)	$\delta^{13}C$ ~ DEPTH + (lon,lat)	1	35	60.1	0.555
2. Nitrogen ($\delta^{15}N$)					
(a) Community scale	$\delta^{15}N$ ~ CHLa + BotTemp + (lon,lat)	2	114	42.3	0.409
(b) Benthic primary producers (group 2)	$\delta^{15}N$ ~ seaHab + (lon,lat)	1	23	90.6	0.888
(c) Pelagic/demersal/benthic fish, demersal cephalopods & macrobenthos carnivores (group 4)	$\delta^{15}N$ ~ CHLa + (lon,lat)	1	48	60.5	0.567
(d) Demersal/benthic fish, demersal cephalopods & macrobenthos carnivores (group 5)	$\delta^{15}N$ ~ seaHab + (lon,lat)	1	50	64.1	0.604
(e) Pelagic/demersal fish & demersal cephalopods (group 6)	$\delta^{15}N$ ~ CHLa + DEPTH + BotTemp + (lon,lat)	3	33	82.0	0.796
(f) Demersal predatory fish (group 7)	$\delta^{15}N$ ~ CHLa + (lon,lat)	1	25	49.0	0.427
(g) Demersal/benthic fish & macrobenthos carnivores (group 8)	$\delta^{15}N$ ~ BotTemp + seaHab + (lon,lat)	2	35	61.6	0.566

% dev, percent deviance explained by model; N. obs, number of sampling locations; N. terms, number of terms.

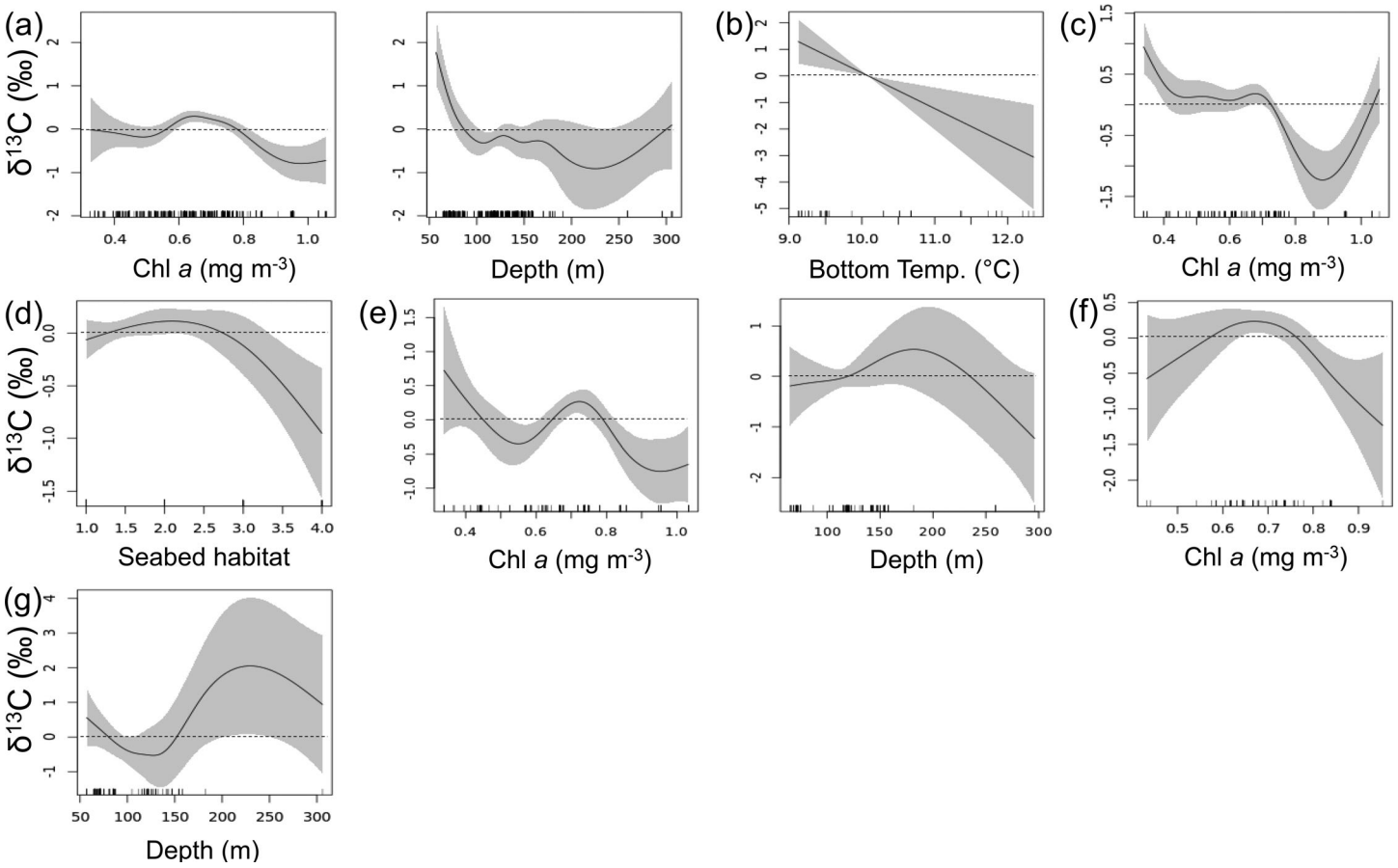

Fig 4. Predicted $\delta^{13}C$ in relation to the most explanatory environmental parameters (unscaled and uncentred) for (**a**) community scale models and (**b–g**) trophic group models. Solid lines show the prediction of a GAM fit to a Gaussian distribution. (**b**) Group 2, (**c**) Group 4, (**d**) Group 5, (**e**) Group 6, (**f**) Group 7, and (**g**) Group 8. Shading represents the 95% confidence interval for predictions. Black bars show the distribution of observations.

which corresponded well to waters over the outer shelf (Fig. 1a,c). Chlorophyll *a* concentrations was common to three groups (groups 4, 6, and 7), but the shape of the response curves varied between groups (Fig. 4c,e,f). Group 4 showed higher $\delta^{13}C$ values, on average, in areas of low chlorophyll *a* (< 0.4 mg m^{-3}), which corresponded well with the northern shelf edge (~ 160 m depth, Fig. 1a,d). For group 7, a positive association with higher $\delta^{13}C$ values was evident at moderate chlorophyll *a* (0.6 and 0.8 mg m^{-3}, Fig. 4c), corresponding with the outer shelf. Group 6 was influenced by chlorophyll *a* and depth (Fig. 4e); higher $\delta^{13}C$ values, on average, were predicted in areas of low (< 0.45 mg m^{-3}) and moderate chlorophyll *a* (0.6 and 0.8 mg m^{-3}) and with deeper relative water depths (> 120 and < 260 m depth), corresponding to the northern shelf edge and outer shelf of the Celtic Sea, respectively (Fig. 1a,d). For group 5, the best model included only seabed habitat (Fig. 4d), with a higher probability of elevated $\delta^{13}C$ values in waters over mud to muddy sand, and sand (Fig. 1b). The $\delta^{13}C$ values of group 8 were influenced by depth (Fig. 4g), with higher $\delta^{13}C$ values, on average, in areas with shallow (< 80 m) and deeper (> 150–170 m) relative water depths, which in this study corresponded well with stations surveying the northeast inner shelf and the deeper waters over Jones Bank and northern shelf edge, respectively (Fig. 1a).

For $\delta^{15}N$, the models fitted on groups 2, 4–8 had good predictive ability with percentage of deviance explained ranging from 49.0% to 90.6% (Table 2). For each group, the best model fitted to $\delta^{15}N$ included between one and three predictor variables (Table 2). Chlorophyll *a* concentrations was common to groups 4, 6, and 7 (Fig. 5c,e,f). A positive association with higher $\delta^{15}N$ values evident between a chlorophyll *a* of 0.6 and 0.8 mg m^{-3} for groups 4 and 7 (Fig. 5c,f). Group 6 was strongly influenced by chlorophyll *a*, depth and bottom temperature (Fig. 5e), with higher $\delta^{15}N$ values, on average, in areas of low (0.5 mg m^{-3}) and moderate chlorophyll *a* (0.6 mg m^{-3} and 0.8 mg m^{-3}) with shallow (< 80 m) and deeper water depths (150 m) and warmer bottom temperatures (> 10.5°C), corresponding to the northern shelf edge, outer shelf and southern areas of the Celtic Sea (Fig. 1a,b,c). Groups 2 and 5 were strongly influenced by seabed habitat, but the response curves differed between groups (Fig. 5b,d). For group 5, a

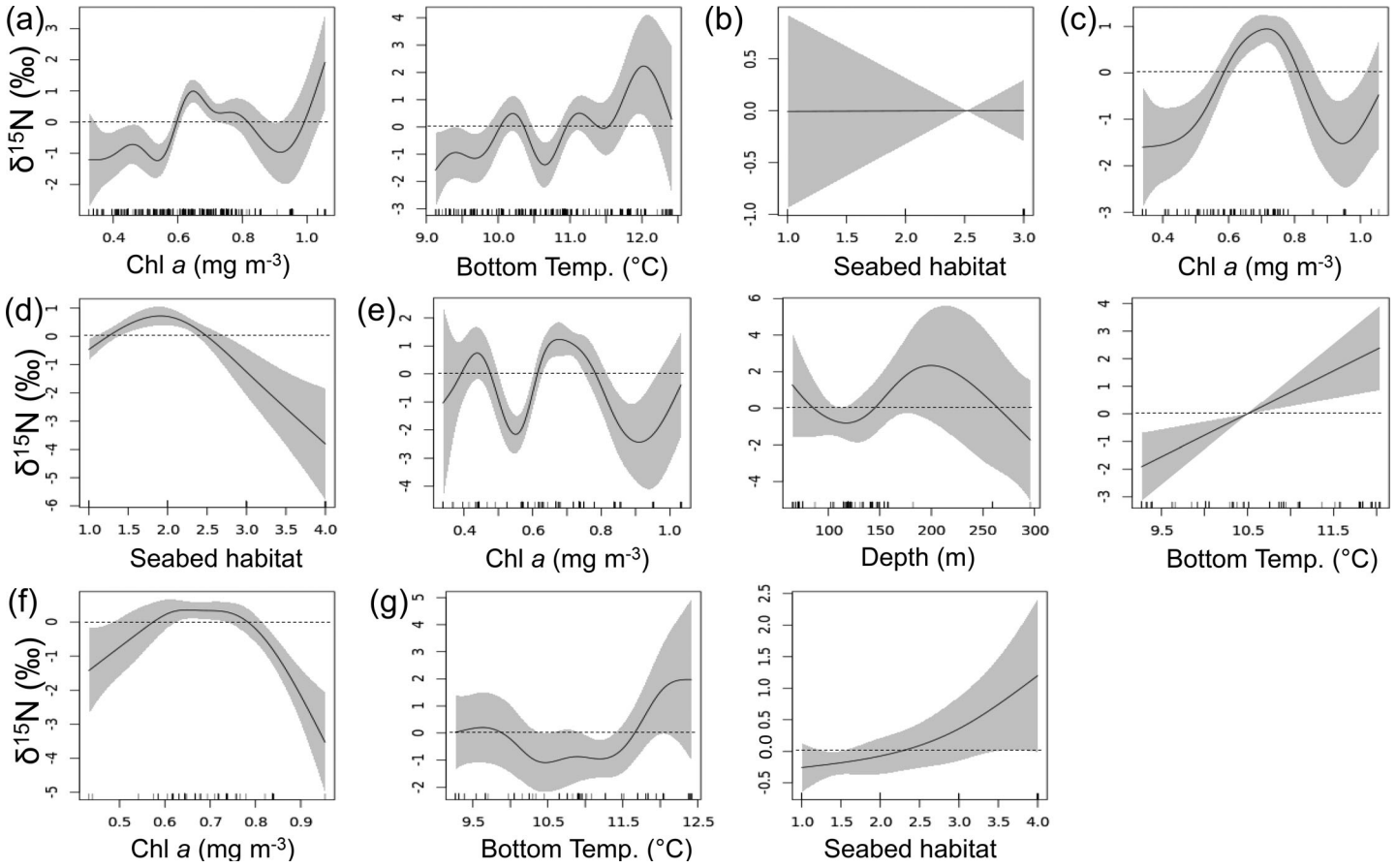

Fig 5. Predicted $\delta^{15}N$ in relation to the most explanatory environmental parameters (unscaled and uncentred) for (**a**) community scale models and (**b**–**g**) trophic group models. Solid lines show the prediction of a GAM fit to a Gaussian distribution. (**b**) Group 2, (**c**) group 4, (**d**) group 5, (**e**) group 6, (**f**) group 7, and (**g**) group 8. Shading represents the 95% confidence interval for predictions. Black bars show the distribution of observations.

positive association with higher $\delta^{15}N$ values was evident in waters over sand (Fig. 1b), while group 2 showed a similar probability of higher or lower $\delta^{15}N$ values in areas over mud to muddy sand, sand and coarse substrate (Fig. 1b).The $\delta^{15}N$ values of group 8 consumers were influenced by bottom temperature and seabed habitat (Fig. 5g), with higher $\delta^{15}N$ values, on average, in areas with warmer bottom temperatures ($> 11.7°C$) and with coarse substrate and mixed sediment (Fig. 1b,c), corresponding to the northeast inner shelf (< 80 m depth; Fig. 1b,c).

Overlap indices of trophic groups in relation to the environment

Overall, two of the strongest biophysical influences associated with trophic group structure were chlorophyll *a* and depth; both $\delta^{13}C$ and $\delta^{15}N$ were generally predicted to be higher in shallow areas (< 80 m depth) of chlorophyll *a* higher than 0.6 mg m^{-3}. To explore underlying species assembly processes at different spatial scales, we compared two spatial areas representing low and high chlorophyll *a* conditions and shallow and deep waters. The spatial comparison was performed for four trophic groups with enough data (Fig. 6). Chlorophyll *a* concentrations had little structuring effect on isotopic niche space among group 4, but was important for pelagic and demersal fish and cephalopods (group 6) and for demersal predatory fish in group 7 (Fig. 6a–c). Group 4 had similar isotope niche area in high (> 0.6 mg m^{-3}) and low (< 0.6 mg m^{-3}) chlorophyll *a* areas. The degree of isotopic overlap (similarity and nestedness) between areas was much larger in group 4 compared to group 7 (Fig. 6a,c). The responses of these metrics are interpretable on the $\delta^{13}C$ axis, which corresponds to changes in primary producers isotopic compositions supporting the food web. For group 4, there was significant overlap on the $\delta^{13}C$ axis between areas for the cephalopod *Sepiola* sp., mackerel (*S. scombrus*), and sardine (*Sardina pilchardus*, Fig. 6a). For group 7, isotopic overlap metrics were likely influenced by whiting (*M. merlangus*) which occupied a different part of the isotopic space on both $\delta^{13}C$ and $\delta^{15}N$ axis in low compared to high chlorophyll *a* conditions (Fig. 6c). The structure of trophic group 6 was altered in high chlorophyll *a* compared to low chlorophyll *a* areas, with an absence of overlap on both $\delta^{13}C$ and $\delta^{15}N$

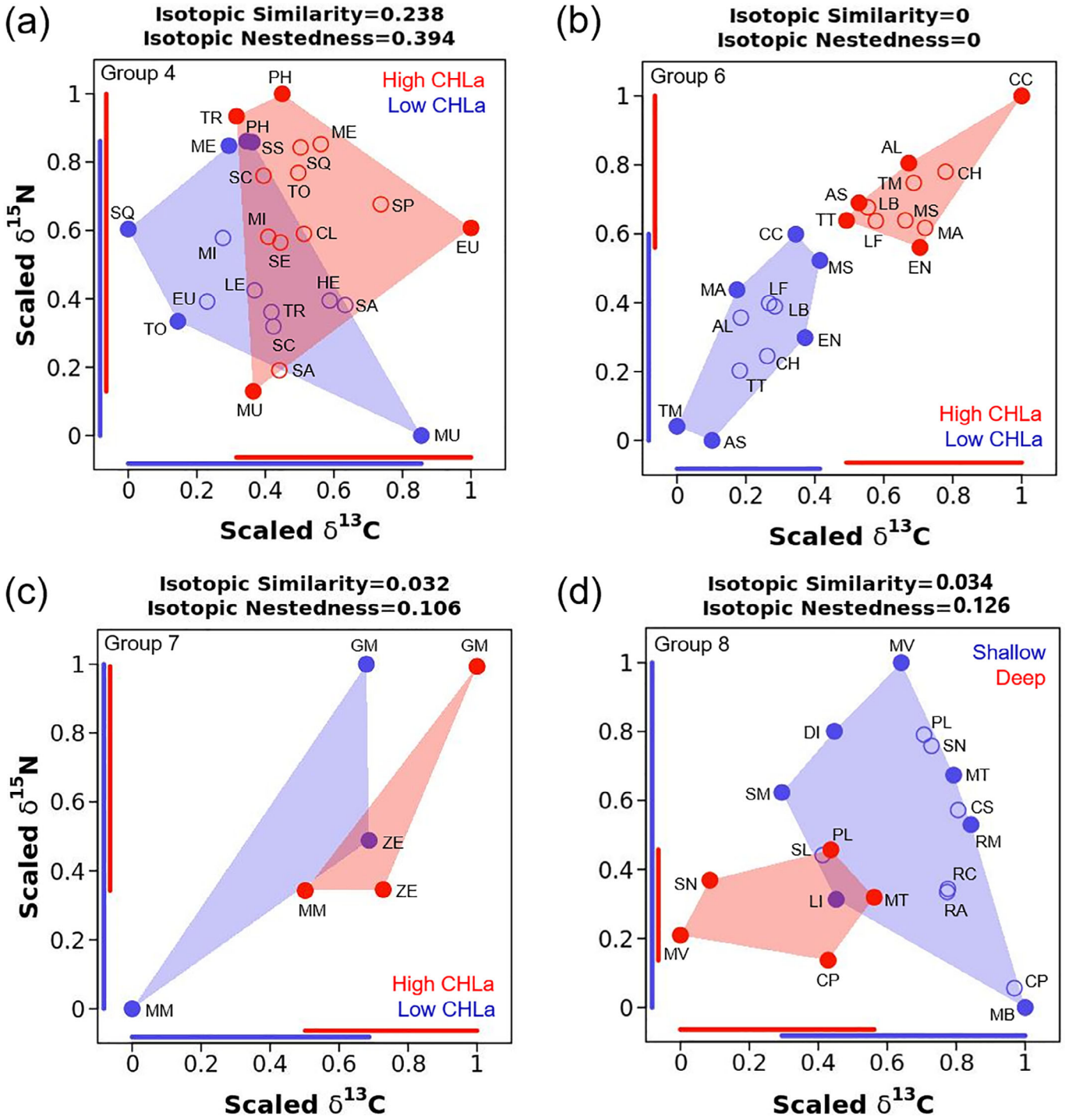

Fig 6. Effect of environmental conditions on isotopic overlap metrics (similarity and nestedness) calculated at trophic group levels. (**a**–**c**) Effect of high (red) and low (blue) chlorophyll *a* concentration on trophic groups 4 "Pelagic/demersal/benthic fish, demersal cephalopods & macrobenthos carnivores", 6 "Pelagic/demersal fish & demersal cephalopods" and 7 "Demersal predatory fish" and (**d**) of water depth (shallow: Blue; deep: Red) on trophic group 8 "Demersal/benthic fish & macrobenthos carnivores". Niches are presented in a scaled (0–1), two-dimensional isotopic space. Scientific names corresponding to species codes are given in Table 1.

axis, but the size of niche space did not vary between areas (Fig. 6b). Change in trophic structure with chlorophyll *a* conditions was largely influenced by poor cod (*T. minutus*), red gurnard (*Chelidonichthys cuculus*), argentine (*Argentina sphyraena*), European common squid (*Alloteuthis* sp.), and horse mackerel (*T. trachurus*) which showed the highest degree

of isotopic separation between high and low chlorophyll *a* areas.

The structuring effect of depth on isotopic niche size was strong in benthic feeding species (Fig. 6d) with minimal isotopic overlap (based on convex hull area) on both the $\delta^{13}C$ and $\delta^{15}N$ axis. Isotopic functional space (i.e., the size of the convex hull area) was three times smaller in deeper waters compared to shallow waters, showing broadened overall isotopic niche space occupied by benthic feeding species. Accordingly, distance between the species points was greater in shallow compared to deeper waters indicating lower trophic redundancy (i.e., higher Isotopic Uniqueness) among species (Fig. 6d; Table S2). Thus, both overlap metrics indicated that the species trophic ecology was more divergent in shallow coastal waters compared with the more clustered species niches in deeper waters (Fig. 6d).

Discussion

Food web structure in the Celtic Sea

The Celtic Sea food web is characterized by four trophic levels and two energy pathways based on different carbon sources (primary producer and detrital-based), suggesting a classical community-structure for a temperate coastal ecosystem (Davenport and Bax 2002; le Loc'h et al. 2008; Kopp et al. 2015). The four trophic levels, from primary consumers (trophic level 2) to the top fish predator (Atlantic cod, *G. morhua*, trophic level 4.4), agrees with previous estimates in the Celtic Sea (Pinnegar et al. 2002), and were comparable to food chain lengths reported from other Northeast Atlantic temperate marine ecosystems (le Loc'h et al. 2008; Kopp et al. 2015; Silberberger et al. 2018) and more widely (Vander Zanden and Fetzer 2007). The range of carbon sources used by primary consumers sampled in the present study is consistent with previously reported ranges for zooplankton (namely copepods) and bivalve mollusks (*P. maximus*) from other Northeast Atlantic coastal waters, including in the Bay of Biscay (le Loc'h et al. 2008) and English Channel (Kopp et al. 2015). Due to bacterial remineralization, benthic ecosystem components are often enriched in the heavy isotopes of carbon (and sometimes nitrogen) compared to fresh, pelagic production. Thus, zooplankton feeding directly on particulate organic matter (POM) are relatively depleted in ^{13}C compared to filter-feeding bivalve mollusks.

Our results, related to the sampling gear used (demersal trawl GOV), showed that the Celtic Sea is characterized by a particularly high abundance of small fish feeding on zooplankton and hyperbenthos known for their vertical migrations and pelagic or demersal predatory fish feeding on small fish and crustaceans. This demonstrates that a substantial proportion of biomass at mid-trophic levels, and by inference production, in the Celtic Sea is supported by production channeled through the pelagic pathway, ultimately fueling large demersal fish at the top of the food web. Besides this, the benthic pathway can be discerned from less depleted ^{13}C compositions of benthic and demersal fish feeding on benthic invertebrates at a low trophic level, to crustacean decapods (e.g., *brachyura* and anomura) at a higher trophic level. The relatively low biomass of benthic- compared to pelagic-feeding fishes suggests that this pathway is less structuring than the pelagic one. It must be acknowledged however, that inferences about the emerging patterns within and across energy pathways are tentative as the biomasses of benthic organisms may have been underestimated due to the sampling gear used in this study. Including all components of an ecosystem (i.e., benthic and pelagic invertebrates, and at least fish), whether through the direct collection of all groups or the development of accurate proxies (e.g., Day et al. 2020), is a major topic in current research, particularly in the context of integrated management of marine systems (Seibold et al. 2018). Nevertheless, in these waters benthic ecosystem components are more or less directly coupled to pelagic primary production, as observed for neighboring environments with similar depths, i.e., the North Sea (Duffill Telsnig et al. 2019) or the Bay of Biscay (Lassalle et al. 2011; Cresson et al. 2020). Feeding plasticity of benthic organisms allows them to position themselves on the pelagic pathway. For instance, a recent isotopic investigation showed suspended POM made up 47% of the diet of the Norway lobster *Nephrops norvegicus* (da Silva Santana et al. 2020). In addition, diel vertically migrating prey (calanoid copepods, euphausiids, mysids, fishes) are also likely to play a significant role in the transfer of pelagic production to benthic ecosystem components in this shallow shelf sea environment. More generally, as benthic consumers exhibit a large trophic plasticity, and largely rely on detritus, they are classically considered as the ultimate opportunists. Their trophic features, such as isotopic ratios, can be viewed as proxies of the predominant source of organic matter in the system (Cresson et al. 2020).

In the Celtic Sea, previous studies also demonstrated the importance of pelagic production to fuel fish assemblages, even at mid-water depths (Trueman et al. 2014). Comparison with results obtained from both empirical data and model outputs on neighboring ecosystems highlight the importance of depth as a major factor driving the degree of connectivity between pelagic and benthic systems (i.e., weakening of the pelagic-benthic coupling from coastal to offshore areas) and the stronger oceanic influence for the Celtic Sea. In the shallow English Channel, the food web is marked by stronger benthic pathways (Kopp et al. 2015; Giraldo et al. 2017). On the contrary, the contribution of pelagic production is predominant in the deeper (~ 140 m depth) Bay of Biscay (Lassalle et al. 2011; Cresson et al. 2020). The apparent gaps in niche space between *P. maximus* and the group of "demersal/benthic fish, demersal cephalopods and macrobenthos carnivores" (Fig. 2) would have been partially filled by isotopic compositions of their prey (decapod crustaceans, mysids, polychaetes,

echinoderms and gastropod mollusks) had we been able to obtain sufficient sample sizes and biomass data for this suite of small invertebrates in this food web.

Our results showed that isotopic functional diversity indices mainly differentiate the generalist consumers from zooplankton consumers, revealing a trophic specialization. The isotopic divergence index indicates a high degree of niche differentiation within the food web. Noticeably, it is in agreement with the mosaic of different seabed habitats that provide complex microhabitat structures for epibenthic assemblages in the Celtic Sea (Ellis et al. 2013). This suggests that the habitat is responsible for the differences in diet width between consumers (probably with lower prey diversity in the pelagic habitat). Trophic specialization occurs more often in predator populations regulated by resources (Estes et al. 2011), and may include the coupling of food resources that are also compartmentalized in space (McCann et al. 2005). For example, in an oligotrophic lake system, the use of distinct habitats in a generalist freshwater predator (Eurasian perch *Perca fluviatilis*) led to intrapopulation niche partitioning between pelagic and littoral subpopulations (Quevedo et al. 2009). In addition to the results obtained for isotopic divergence, low isotopic evenness and uniqueness values showed that the food web is composed of clusters of species, revealing more dietary overlap and thus more competition for the same resource at intermediate trophic levels. Ashton et al. (2010) found the existence of plasticity in resource use among dominant species provides a mechanism by which species with broadly overlapping resource use might coexist. In the Celtic Sea ecosystem, higher specialization among generalist species feeding in different microhabitats may therefore provide opportunities to maximize resource use (i.e., niche complementarity) and thus augment productivity. Indeed, Day et al. (2019) found distinct feeding niches and strategies within four dominant predatory fishes, which effectively limit interspecific competition in the area. Consistent with the results obtained for the other metrics, low isotopic dispersion showed average trophic diversity in the food web is low due to substantial reductions in the abundance of top predator fish due to intense fishing in the area, which has cascaded into an increased abundance of small, pelagic and demersal fishes feeding lower in the food web over time (Pinnegar et al. 2002; Hernvann and Gascuel 2020).

It is predicted that more complex food webs will be more resilient to environmental changes due to greater trophic redundancy that can buffer against species loss (Sanders et al. 2018). The high trophic redundancy at intermediate trophic levels reported here probably offers great resistance to disturbances (Walters and Post 2008). In the Celtic Sea, relations between taxa and the environment have remained stable over the past two decades (Mérillet et al. 2019), perhaps due to this high trophic redundancy in the system or the fact that the ecosystem has been shaped by fishing for such a long period of time now and therefore has adapted to an overall stable state. However, with ongoing climate change, increased bottom temperature in the area is likely to substantially alter the distribution of taxa in the coming years, especially cold-water taxa (Mérillet et al. 2019). This in turn may lead to a decrease in prey diversity and thus energy transfer within the ecosystem, and consequently on the food availability for higher trophic levels. While all facets of isotopic diversity are important indicators of the functioning of ecological systems, isotopic divergence, evenness and uniqueness indices may be most informative when investigating the degree of habitat coupling mediated by predators (McCann et al. 2005), particularly in ecologically complex food webs.

Biological and physical drivers of trophic variability

Knowing which biophysical variables drive changes in the main functional components is key to understanding variability in food web structure in the Celtic Sea. Studies of fish and invertebrate abundance and species distributions recognized that depth, chlorophyll *a* concentrations and bottom temperature influence assemblages of demersal communities in the Celtic Sea alongside changes in fisheries pressures (Mérillet et al. 2019), while bathymetry, bottom temperature and salinity were found to be the main drivers structuring planktonic assemblages (Haberlin et al. 2019). Fluctuations in the strength and properties of these processes may therefore have a major impact on the stability of the functional composition and spatial organization of the food web.

In this study, we demonstrated that in the Celtic Sea, chlorophyll *a* concentrations were strongly associated with higher $\delta^{13}C$ and $\delta^{15}N$ values at moderate levels of chlorophyll *a* (> 0.6 and < 0.8 mg m^{-3}) congruent with colder bottom temperatures ($< 10^{\circ}C$), and with higher $\delta^{13}C$ and $\delta^{15}N$ values at the highest chlorophyll *a* levels (> 1.0 mg m^{-3}) in areas with warmer bottom temperatures ($> 11.5^{\circ}C$) and shallower bathymetry (< 80 m depth). Chlorophyll *a* concentrations decrease rapidly from inner shelf areas on the shelf, and the seasonal cycle of primary production is tightly coupled to the change in vertical water column structure (Wihsgott et al. 2019). In coastal waters, as opposed to offshore areas where the $\delta^{13}C$ and $\delta^{15}N$ baseline may be relatively stable (Jennings and Warr 2003; MacKenzie et al. 2014), there are greater temporal variations in bottom temperature and salinity, which has been shown to alter $\delta^{13}C$ and $\delta^{15}N$ values at the base of the food web, ultimately affecting consumer isotope values (Jennings and van der Molen 2015). These results therefore point to consistent zonal differences in $\delta^{13}C$ and $\delta^{15}N$ values along oligotrophic-to-eutrophic gradients in the Celtic Sea (Marañón et al. 2005), previously observed in oceanic upwelling areas and on continental shelves (e.g., Radabaugh et al. 2013). Correlations between $\delta^{13}C$ and $\delta^{15}N$ and surface concentrations of chlorophyll *a* may be higher over the outer shelf due to resupply of inorganic nutrients from the dark, nutrient-rich bottom waters to the nutrient-depleted surface waters (Wihsgott et al. 2019). Higher

$\delta^{13}C$ and $\delta^{15}N$ values may also be linked to intrusions from the Bristol Channel, Severn Estuary, and the English Channel, which are carried along the inner shelf by wind-driven coastal currents reinforced by density-driven currents associated with seasonal fronts (Uncles 2010). Higher isotopic ratios measured in higher productive conditions may also be linked with increase of downward exports of pelagic production. For example, Ying et al. (2020) recently observed an unexpected mismatch between pelagic production and pelagic contribution. When the production of the pelagic system was low, it contributed substantially to both benthic and pelagic systems, but with low biomass for all functional groups, and high trophic overlap between them. On the contrary, when pelagic production increased, its contribution to benthic groups decreased, along with lower overlap and higher biomasses of benthic fish and crustaceans. This unexpected pattern may be related to increased downward fluxes, that increase benthic secondary production and/or bacterial alteration of organic matter, and an increased importance of the benthic pathway in the whole system that contributes to increased isotopic ratios (Griffiths et al. 2017).

The community scale pattern of spatial trends in $\delta^{13}C$ and $\delta^{15}N$ values is remarkably consistent among trophic groups. This consistency suggests that spatially explicit trends are conserved from the base of the food web into the upper trophic levels. It may suggest that large predatory fishes move only a limited amount in the region as residency of predators and prey is required for spatial trends in isotope values to propagate up the food web (Graham et al. 2010). Five distinct trophic assemblages occur within the Celtic Sea, associated with different chlorophyll *a* concentrations, water depth and bottom temperature: (1) a cold, vertically mixed-water assemblage over the outer shelf characterized by moderate chlorophyll *a* (0.6–0.8 mg m^{-3}). This habitat was the largest and hosts the most diverse assemblage. This is consistent with the findings of Ellis et al. (2013) who found the outer shelf epibenthic assemblage to be the most speciose in the region. Scallops (*P. maximus*) were strongly associated with colder bottom temperatures in the area (< 10°C). While seabed habitat (mud to muddy sand) was the strongest predictor for the group of "demersal/benthic fish, demersal cephalopods and macrobenthos carnivores", which hosted taxa including Norway lobster that are known to predominantly occur in the area (Ellis et al. 2013). This highlights the importance of cold productive environmental conditions in the Celtic Sea (Mérillet et al. 2019), where the availability of optimal prey for predators may lead to higher dietary specialization and stronger habitat coupling (McCann et al. 2005). (2) An oceanic assemblage over the northern shelf edge, characterized by low chlorophyll *a* (< 0.45 mg m^{-3}) and deeper depths (~ 160 m). This habitat comprises a greater diversity of oceanic and neritic taxa, which adds to previous studies in explaining the spatial heterogeneity in taxa distribution in the Celtic Sea (Dolder et al. 2018; Mérillet et al. 2019). (3) A warmer mixed-water assemblage in the southern part of the shelf characterized by deeper depths (> 150 m). Species in this habitat are the most widely distributed across habitats (i.e., northern shelf edge, outer shelf and southern part) in the Celtic Sea. This also highlights the increase in diversity and biomass of taxa in warmer waters in the Celtic Sea. In regions where the fronts separate a warm stratified offshore region from a tidally mixed cooler inshore region, Haberlin et al. (2019) observed a greater gelatinous zooplankton diversity and biomass in the warm water community. Two habitats comprised benthic taxa, which were strongly influenced by depth: (4) a warm, shallow mixed-water assemblage over the northeast inner shelf, and (5) a colder mixed-water assemblage over the central part of the study area contiguous with the Jones Bank, and the shelf edge characterized by deeper waters (> 150 m). The inner shelf assemblage was also strongly associated with coarse sediments and mixed substrate in the area highlighting the importance of these fine-scale, fragmented seabed habitats in generating spatial heterogeneity and structurally complex microhabitats within the ecosystem.

Changes in trophic niches

The structuring effect of chlorophyll *a* concentration on the niche of pelagic ("pelagic/demersal/benthic fish, demersal cephalopods and macrobenthos carnivores") and benthic functional groups ("pelagic/demersal fish and demersal cephalopods" and "demersal predatory fish") clearly differed. This difference may be related to pelagic species that are not plastic, i.e., always belonging to a pelagic-based pathway whatever the level of pelagic production, potentially driven by upward fluxes of matter. In contrast, benthic species are more plastic, whether in their diet, or in the source of matter fueling the benthic pathway. As observed in other systems (Hayden et al. 2019; Ying et al. 2020), increased pelagic production increases downward fluxes, and stimulates benthic production and bacterial activity. In this study, the major niche shift observed for opportunist benthic groups could thus testify to the increased importance of benthic production at two trophic levels.

Water depth strongly influenced isotopic niche space of the benthic functional group of "demersal/benthic fish and macrobenthos carnivores." Isotopic niche area was larger (spanning two trophic levels) in shallow habitats, but not in habitats underlying high primary production or nutrient-rich water masses, suggesting stronger benthic-pelagic trophic coupling in inner shelf habitats. In nearshore habitats where water depth is relatively shallow (< 80 m depth), the daytime thickness of the vertically migrating community is compressed into a shallow layer. This means that pelagic sources are potentially more accessible to benthic consumers, and reciprocally, benthic species more accessible to pelagic consumers, resulting in complex systems with multiple interactions as previously documented in coastal shelf studies (Kopp et al. 2015; Giraldo et al. 2017). In deeper habitats (> 80 m

depth), niche area was much smaller due to the reduction in food sources in less diverse pelagic environments, as expected. We also found a marked difference in the diversity of taxa between shallow and deep water habitats, with the former tending to have a greater diversity of more coastal species that were characteristic of inshore waters. Decreasing variability of isotopic ratios with depth was previously found in fish and invertebrates in the eastern English Channel (Kopp et al. 2015). In this study, decreasing variability of isotopic ratios from shallow to deeper habitats was associated with changes in hydrodynamics and seabed habitats, as well as to changes in the availability of benthic prey/resources. The results are consistent with the findings of Day et al. (2019) who observed a decrease in diet spectra of demersal fish predators from shallow to deeper depths in the Celtic Sea. The importance of hydrodynamics and different sedimentary types on the spatial structuring of epibenthos in the Celtic Sea has been previously highlighted (Ellis et al. 2013).

Conclusion

This study significantly advances our understanding of the drivers of trophic structure and functioning of communities in the Celtic Sea, a large productive shelf ecosystem that supports important fisheries in the region (Mateo et al. 2017; Moore et al. 2019). Prior to this study, no information has been available on the overall structure of the food web in relation to the biophysical environment, yet understanding of the underlying processes structuring trophic assemblages and the wider Celtic Sea ecosystem is central to inform effective resource management. Our results show that the Celtic Sea food web forms a continuum of four trophic levels with trophic groups spread across two trophic pathways based on pelagic (primary producer based) and benthic (detrital-based) systems. Four biomass-weighted isotopic diversity indices (isotopic divergence, dispersion, evenness, and uniqueness) provided indicators on the status of the system, showing a relatively complex food web with high trophic redundancy at intermediate trophic levels suggesting resilience to disturbances. Five distinct trophic assemblages were found in the Celtic Sea associated with different environmental conditions, suggesting that depth and intensity of pelagic production are major drivers of trophic structure and functioning of communities and requires further investigation. This research also highlights the importance of cold productive conditions in the Celtic Sea and adds to previous studies in explaining the spatial heterogeneity in taxa distribution on the shelf, e.g., fish (Dolder et al. 2018; Mérillet et al. 2019), zooplankton (Haberlin et al. 2019), and epibenthic community assemblages (Ellis et al. 2013). The structuring effect of depth on isotopic niche size in benthic functional groups highlights the necessity to identify underlying species assembly processes at different spatial scales to inform effective resource management.

References

Agnetta, D., F. Badalamenti, F. Colloca, and others. 2019. Benthic-pelagic coupling mediates interactions in Mediterranean mixed fisheries: An ecosystem modeling approach. PLoS One **14**: e0210659.

Ashton, I. W., A. E. Miller, W. D. Bowman, and K. N. Suding. 2010. Niche complementarity due to plasticity in resource use: Plant partitioning of chemical N forms. Ecology **91**: 3252–3260. doi:10.1890/09-1849.1

Barnes, C., S. Jennings, and J. T. Barry. 2009. Environmental correlates of large-scale spatial variation in the δ13C of marine animals. Estuar. Coast. Shelf Sci. **81**: 368–374. doi: https://doi.org/10.1016/j.ecss.2008.11.011

Blanchard, F., and F. Vandermeirsch. 2005. Warming and exponential abundance increase of the subtropical fish *Capros aper* in the Bay of Biscay (1973–2002). C. R. Biol. **328**: 505–509. doi:https://doi.org/10.1016/j.crvi.2004.12.006

Borcard, D., F. Gillet, and P. Legendre. 2018. Numerical ecology with R, Springer, Cham, Switzerland.

Burnham, K. P., and D. R. Anderson. 2002. Model selection and multimodel inference: A practical information theoretic approach, 2nd ed. New York: Springer.

Cresson, P., T. Chouvelon, P. Bustamante, and others. 2020. Primary production and depth drive different trophic structure and functioning of fish assemblages in French marine ecosystems. Prog. Oceanogr. **186**: 102343. doi:https://doi.org/10.1016/j.pocean.2020.102343

Cucherousset, J., and S. Villéger. 2015. Quantifying the multiple facets of isotopic diversity: New metrics for stable isotope ecology. Ecol. Indic. **56**: 152–160. doi:10.1016/j.ecolind.2015.03.032

da Silva Santana, C. A., A. M. Wieczorek, P. Browne, C. T. Graham, and A. M. Power. 2020. Importance of suspended particulate organic matter in the diet of *Nephrops norvegicus* (Linnaeus, 1758). Sci. Rep. **10**: 3387. doi:10.1038/s41598-020-60367-x

Darnaude, A. M., C. Salen-Picard, N. V. C. Polunin, and M. L. Harmelin-Vivien. 2004. Trophodynamic linkage between river runoff and coastal fishery yield elucidated by stable isotope data in the Gulf of Lions (NW Mediterranean). Oecologia **138**: 325–332. doi:10.1007/s00442-003-1457-3

Davenport, S. R., and N. J. Bax. 2002. A trophic study of a marine ecosystem off southeastern Australia using stable isotopes of carbon and nitrogen. Can. J. Fish. Aquat. Sci. **59**: 514–530. doi:10.1139/f02-031

Day, L., D. Kopp, M. Robert, and H. le Bris. 2019. Trophic ecology of large gadiforms in the food web of a continental shelf ecosystem. Prog. Oceanogr. **175**: 105–114. doi:10.1016/j.pocean.2019.03.007

Day, L., H. le Bris, E. Saulnier, L. Pinsivy, and A. Brind'Amour. 2020. Benthic prey production index estimated from trawl survey supports the food limitation hypothesis in coastal fish nurseries. Estuar. Coast. Shelf Sci. **235**: 106594. doi: https://doi.org/10.1016/j.ecss.2020.106594

Dolder, P. J., J. T. Thorson, and C. Minto. 2018. Spatial separation of catches in highly mixed fisheries. Sci. Rep. **8**: 13886. doi:10.1038/s41598-018-31881-w

Duffill Telsnig, J. I., S. Jennings, A. C. Mill, N. D. Walker, A. C. Parnell, and N. V. C. Polunin. 2019. Estimating contributions of pelagic and benthic pathways to consumer production in coupled marine food webs. J. Anim. Ecol. **88**: 405–415. doi:10.1111/1365-2656.12929

Duhamel, E., M. Salaun, and L. Pawlowski. 2014. EVHOE 2014 cruise, RV Thalassa.

Eddy, T. D., J. R. Bernhardt, J. L. Blanchard, and others. 2020. Energy flow through marine ecosystems: Confronting transfer efficiency. Trends Ecol. Evol. **36**: 76–86. doi:10.1016/j.tree.2020.09.006

Ellis, J. R., I. Martinez, G. J. Burt, and B. E. Scott. 2013. Epibenthic assemblages in the Celtic Sea and associated with the Jones Bank. Prog. Oceanogr. **117**: 76–88. doi:https://doi.org/10.1016/j.pocean.2013.06.012

Estes, J. A., J. Terborgh, J. S. Brashares, and others. 2011. Trophic downgrading of planet earth. Science (80–.) **333**: 301–306. doi:10.1126/science.1205106

Giraldo, C., B. Ernande, P. Cresson, D. Kopp, M. Cachera, M. Travers-Trolet, and S. Lefebvre. 2017. Depth gradient in the resource use of a fish community from a semi-enclosed sea. Limnol. Oceanogr. **62**: 2213–2226. doi:10.1002/lno.10561

Gohin, F., B. Saulquin, H. Oger-Jeanneret, L. Lozac'h, L. Lampert, A. Lefebvre, P. Riou, and F. Bruchon. 2008. Towards a better assessment of the ecological status of coastal waters using satellite-derived chlorophyll-a concentrations. Remote Sens. Environ. **112**: 3329–3340. doi:https://doi.org/10.1016/j.rse.2008.02.014

Graham, B. S., P. L. Koch, S. D. Newsome, K. W. McMahon, and D. Aurioles. 2010. Using Isoscapes to trace the movements and foraging behavior of top predators in oceanic ecosystems, p. 299–318.*In* J. B. West, G. J. Bowen, T. E. Dawson, and K. P. Tu [eds.], Isoscapes: Understanding movement, pattern, and process on earth through isotope mapping. Springer Netherlands.

Griffiths, J. R., M. Kadin, F. J. A. Nascimento, and others. 2017. The importance of benthic–pelagic coupling for marine ecosystem functioning in a changing world. Glob. Chang. Biol. **23**: 2179–2196. doi:10.1111/gcb.13642

Habel, K., R. Grasman, R. B. Gramacy, P. Mozharovskyi, and D. C. Sterratt. 2019. geometry: Mesh Generation and Surface Tessellation.

Haberlin, D., R. Raine, R. McAllen, and T. K. Doyle. 2019. Distinct gelatinous zooplankton communities across a dynamic shelf sea. Limnol. Oceanogr. **64**: 1802–1818. doi:10.1002/lno.11152

Hayden, B., C. Harrod, S. M. Thomas, and others. 2019. From clear lakes to murky waters: Tracing the functional response of high-latitude lake communities to concurrent 'greening' and 'browning'. Ecol. Lett. **22**: 807–816. doi:10.1111/ele.13238

Hernvann, P.-Y., and D. Gascuel. 2020. Exploring the impacts of fishing and environment on the Celtic Sea ecosystem since 1950. Fish. Res. **225**: 105472. doi:https://doi.org/10.1016/j.fishres.2019.105472

Hu, C., Z. Lee, and B. Franz. 2012. Chlorophyll aalgorithms for oligotrophic oceans: A novel approach based on three-band reflectance difference. J. Geophys. Res. Ocean. **117**: C01011. doi:10.1029/2011JC007395

ICES. 2015. Report of the International Bottom Trawl Survey Working Group (IBTSWG), 23–27 March 2015.

Jennings, S., and J. van der Molen. 2015. Analysis: Estimation and uncertainty. ICES J. Mar. Sci. **72**: 2289–2300.

Jennings, S., and K. J. Warr. 2003. Environmental correlates of large-scale spatial variation in the δ15N of marine animals. Mar. Biol. **142**: 1131–1140. doi:10.1007/s00227-003-1020-0

Kopp, D., S. Lefebvre, M. Cachera, M. C. Villanueva, and B. Ernande. 2015. Reorganization of a marine trophic network along an inshore-offshore gradient due to stronger pelagic-benthic coupling in coastal areas. Prog. Oceanogr. **130**: 157–171. doi:10.1016/j.pocean.2014.11.001

Kopp, D., M. Robert, and L. Pawlowski. 2018. Characterization of food web structure of the upper continental slope of the Celtic Sea highlighting the trophic ecology of five deep-sea fishes. J. Appl. Ichthyol. **34**: 73–80. doi:10.1111/jai.13544

Lassalle, G., J. Lobry, F. le Loc'h, and others. 2011. Lower trophic levels and detrital biomass control the Bay of Biscay continental shelf food web: Implications for ecosystem management. Prog. Oceanogr. **91**: 561–575. doi:https://doi.org/10.1016/j.pocean.2011.09.002

Layman, C. A., M. S. Araujo, R. Boucek, and others. 2012. Applying stable isotopes to examine food-web structure: An overview of analytical tools. Biol. Rev. **87**: 545–562. doi:https://doi.org/10.1111/j.1469-185X.2011.00208.x

le Loc'h, F., C. Hily, and J. Grall. 2008. Benthic community and food web structure on the continental shelf of the Bay of Biscay (North Eastern Atlantic) revealed by stable isotopes analysis. J. Mar. Syst. **72**: 17–34. doi:10.1016/j.jmarsys.2007.05.011

Leaute, J.-P., L. Pawlowski, and M. Salaun. 2015. EVHOE 2015 cruise, RV Thalassa.

Leaute, J.-P., L. Pawlowski, and F. Garren. 2016. EVHOE 2016 cruise, RV Thalassa.

Lorrain, A., Y.-M. Paulet, L. Chauvaud, N. Savoye, A. Donval, and C. Saout. 2002. Differential δ13C and δ15N signatures among scallop tissues: Implications for ecology and physiology. J. Exp. Mar. Bio. Ecol. **275**: 47–61. doi:https://doi.org/10.1016/S0022-0981(02)00220-4

MacKenzie, K. M., C. Longmore, C. Preece, C. H. Lucas, and C. N. Trueman. 2014. Testing the long-term stability of marine isoscapes in shelf seas using jellyfish tissues. Biogeochemistry **121**: 441–454. doi:10.1007/s10533-014-0011-1

Marañón, E., P. Cermeño, and V. Pérez. 2005. Continuity in the photosynthetic production of dissolved organic carbon

from eutrophic to oligotrophic waters. Mar. Ecol. Prog. Ser. **299**: 7–17.

Martinez, I., J. R. Ellis, B. Scott, and A. Tidd. 2013. The fish and fisheries of Jones Bank and the wider Celtic Sea. Prog. Oceanogr. **117**: 89–105. doi:https://doi.org/10.1016/j.pocean.2013.03.004

Mateo, M., L. Pawlowski, and M. Robert. 2017. Highly mixed fisheries: Fine-scale spatial patterns in retained catches of French fisheries in the Celtic Sea. ICES J. Mar. Sci. **74**: 91–101. doi:10.1093/icesjms/fsw129

McCann, K. S., J. B. Rasmussen, and J. Umbanhowar. 2005. The dynamics of spatially coupled food webs. Ecol. Lett. **8**: 513–523. doi:10.1111/j.1461-0248.2005.00742.x

McLean, M., D. Mouillot, M. Lindegren, S. Villéger, G. Engelhard, J. Murgier, and A. Auber. 2019. Fish communities diverge in species but converge in traits over three decades of warming. Glob. Chang. Biol. **25**: 3972–3984. doi:10.1111/gcb.14785

Mérillet, L., D. Kopp, M. Robert, M. Mouchet, and S. Pavoine. 2019. Environment outweighs the effects of fishing in regulating demersal community structure in an exploited marine ecosystem. Glob. Chang. Biol. **26**: 2106–2119. doi:10.1111/gcb.14969

Moore, C., S. Davie, M. Robert, L. Pawlowski, P. Dolder, and C. Lordan. 2019. Defining métier for the Celtic Sea mixed fisheries: A multiannual international study of typology. Fish. Res. **219**: 105310. doi:https://doi.org/10.1016/j.fishres.2019.105310

National Geophysical Data Center. 2006. 2-minute Gridded Global Relief Data (ETOPO2) v2.doi:10.7289/V5J1012Q

Newsome, S. D., C. Martinez del Rio, S. Bearhop, and D. L. Phillips. 2007. A niche for isotopic ecology. Front. Ecol. Environ. **5**: 429–436. doi:10.1890/060150.1

Oksanen, J., F. Oksanen, G. Blanchet, and others. 2019. vegan: Community Ecology Package.

Paradis, E., and K. Schliep. 2019. ape 5.0: An environment for modern phylogenetics and evolutionary analyses in R. Bioinformatics **35**: 526–528.

Petrik, C. M., C. A. Stock, K. H. Andersen, P. D. van Denderen, and J. R. Watson. 2019. Bottom-up drivers of global patterns of demersal, forage, and pelagic fishes. Prog. Oceanogr. **176**: 102124. doi:https://doi.org/10.1016/j.pocean.2019.102124

Pinnegar, J. K., S. Jennings, C. M. O'Brien, and N. V. C. Polunin. 2002. Long-term changes in the trophic level of the Celtic Sea fish community and fish market price distribution. J. Appl. Ecol. **39**: 377–390. doi:10.1046/j.1365-2664.2002.00723.x

Pinnegar, J. K., V. M. Trenkel, A. N. Tidd, W. A. Dawson, and M. H. Du buit. 2003. Does diet in Celtic Sea fishes reflect prey availability? J. Fish Biol. **63**: 197–212. doi:10.1111/j.1095-8649.2003.00204.x

Populus, J., M. Vasquez, J. Albrecht, and others. 2017. EUSeaMap. A European broad-scale seabed habitat map.

Post, D. M. 2002. Using stable isotopes to estimate trophic position: Models, methods, and assumptions. Ecology **83**: 703–718 10.1890/0012-9658(2002)083[0703:USITET]2.0.CO;2

Post, D. M., C. A. Layman, D. A. Arrington, G. Takimoto, J. Quattrochi, and C. G. Montaña. 2007. Getting to the fat of the matter: Models, methods and assumptions for dealing with lipids in stable isotope analyses. Oecologia **152**: 179–189. doi:10.1007/s00442-006-0630-x

Quevedo, M., R. Svanbäck, and P. Eklöv. 2009. Intrapopulation niche partitioning in a generalist predator limits food web connectivity. Ecology **90**: 2263–2274. doi:10.1890/07-1580.1

R Core Team. 2020. R: A Language and Environment for Statistical Computing. R Foundation for Statistical Computing. Vienna, Austria, URL https://www.R-project.org/.

Radabaugh, K. R., D. J. Hollander, and E. B. Peebles. 2013. Seasonal δ13C and δ15N isoscapes of fish populations along a continental shelf trophic gradient. Cont. Shelf Res. **68**: 112–122. doi:10.1016/j.csr.2013.08.010

Rault, J., H. le Bris, M. Robert, L. Pawlowski, M. Denamiel, and D. Kopp. 2017. Diets and trophic niches of the main commercial fish species from the Celtic Sea. J. Fish Biol. **91**: 1449–1474. doi:10.1111/jfb.13470

Rigolet, C., E. Thiébaut, A. Brind'Amour, and S. F. Dubois. 2015. Investigating isotopic functional indices to reveal changes in the structure and functioning of benthic communities. Funct. Ecol. **29**: 1350–1360. doi:10.1111/1365-2435.12444

Sanders, D., E. Thébault, R. Kehoe, and F. J. van Frank Veen. 2018. Trophic redundancy reduces vulnerability to extinction cascades. Proc. Natl. Acad. Sci. USA **115**: 2419–2424. doi:10.1073/pnas.1716825115

Seibold, S., M. W. Cadotte, J. S. MacIvor, S. Thorn, and J. Müller. 2018. The necessity of multitrophic approaches in community ecology. Trends Ecol. Evol. **33**: 754–764. doi:https://doi.org/10.1016/j.tree.2018.07.001

Silberberger, M. J., P. E. Renaud, I. Kröncke, and H. Reiss. 2018. Food-web structure in four locations along the European shelf indicates spatial differences in ecosystem functioning. Front. Mar. Sci. **5**: 119.

Smyntek, P. M., M. A. Teece, K. L. Schulz, and S. J. Thackeray. 2007. A standard protocol for stable isotope analysis of zooplankton in aquatic food web research using mass balance correction models. Limnol. Oceanogr. **52**: 2135–2146. doi:10.4319/lo.2007.52.5.2135

Sumner, M. D. 2019. raadtools: Tools for synoptic environmental spatial data.

Trueman, C. N., G. Johnston, B. O'Hea, and K. M. MacKenzie. 2014. Trophic interactions of fish communities at midwater depths enhance long-term carbon storage and benthic production on continental slopes. Proc. R. Soc. B Biol. Sci. **281**: 20140669. doi:10.1098/rspb.2014.0669

Uncles, R. J. 2010. Physical properties and processes in the Bristol Channel and Severn estuary. Mar. Pollut. Bull. **61**: 5–20. doi:10.1016/j.marpolbul.2009.12.010

Vander Zanden, J. M., and W. W. Fetzer. 2007. Global patterns of aquatic food chain length. Oikos **116**: 1378–1388. doi: 10.1111/j.0030-1299.2007.16036.x

Vaz, S., A. Auber, F. Coppin, and others. 2019. Benthic invertebrates' by-catches in Ifremer bottom trawl surveys in the English Channel and southern North Sea: 2006–2018 observations. SEANOE.

Walters, A. W., and D. M. Post. 2008. An experimental disturbance alters fish size structure but not food chain length in streams. Ecology **89**: 3261–3267. doi:10.1890/08-0273.1

Wihsgott, J. U., J. Sharples, J. E. Hopkins, E. M. S. Woodward, T. Hull, N. Greenwood, and D. B. Sivyer. 2019. Observations of vertical mixing in autumn and its effect on the autumn phytoplankton bloom. Prog. Oceanogr. **177**: 102059. doi:https://doi.org/10.1016/j.pocean.2019.01.001

Wood, S. N. 2017. Generalized additive models: An introduction with R, 2nd ed. Chapman and Hall/CRC.

Ying, R., Y. Cao, F. Yin, and others. 2020. Trophic structure and functional diversity reveal pelagic-benthic coupling dynamic in the coastal ecosystem of Daya Bay, China. Ecol. Indic. **113**: 106241. doi:https://doi.org/10.1016/j.ecolind.2020.106241

van Denderen P. D., M. Lindegren, B. R. MacKenzie, R. A. Watson, K. H. Andersen 2018. Global patterns in marine predatory fish. Nature Ecology & Evolution **2**: 65–70. doi: 10.1038/s41559-017-0388-z

Acknowledgments

This study was carried out as part of the EATME project supported by France Fillère Pêche and Region Bretagne. P. Cresson is supported by grants from the French government, the Region Haut de France and Ifremer under the framework of the project CPER MARCO 2015–2020. A. Walters is an Adjunct Researcher within the Institute for Marine and Antarctic Studies, University of Tasmania. The authors would like to thank Laurène Mérillet and Pierre-Yves Hernvann for data support and discussions, and the crew onboard the R/V "Thalassa." The authors thank the editor K. David Hambright and two anonymous reviewers for comments that improved previous versions of the manuscript.

Conflict of interest

None declared.

Submitted 17 July 2020
Revised 19 January 2021
Accepted 30 March 2021

Associate editor: Anna Armitage